Searches for Higgs boson pair production in the $hh \to bb\tau\tau$, $\gamma\gamma WW^*$, $\gamma\gamma bb$, $bbbb$ channels with the ATLAS detector

G. Aad *et al.*[*]

(ATLAS Collaboration)

Searches for both resonant and nonresonant Higgs boson pair production are performed in the $hh \to bb\tau\tau$, $\gamma\gamma WW^*$ final states using 20.3 fb^{-1} of pp collision data at a center-of-mass energy of 8 TeV recorded with the ATLAS detector at the Large Hadron Collider. No evidence of their production is observed and 95% confidence-level upper limits on the production cross sections are set. These results are then combined with the published results of the $hh \to \gamma\gamma bb$, $bbbb$ analyses. An upper limit of 0.69 (0.47) pb on the nonresonant hh production is observed (expected), corresponding to 70 (48) times the SM $gg \to hh$ cross section. For production via narrow resonances, cross-section limits of hh production from a heavy Higgs boson decay are set as a function of the heavy Higgs boson mass. The observed (expected) limits range from 2.1 (1.1) pb at 260 GeV to 0.011 (0.018) pb at 1000 GeV. These results are interpreted in the context of two simplified scenarios of the Minimal Supersymmetric Standard Model.

I. INTRODUCTION

The Higgs boson discovered at the LHC in 2012 [1,2] opens a window for testing the scalar sector of the Standard Model (SM) and its possible extensions. Since the discovery, significant progress has been made in measuring its coupling strengths to fermions and vector bosons [3–6] as well as in studying its spin and its charge-conjugate and parity (CP) properties [7,8]. All results are consistent with those expected for the SM Higgs boson (here denoted by h). Within the SM, the existence of the Higgs boson is a consequence of the electroweak symmetry breaking (EWSB). This also predicts self-coupling between Higgs bosons, the measurement of which is crucial in testing the mechanism of EWSB. The self-coupling is one mechanism for Higgs boson pair production as shown in Fig. 1(a). Higgs boson pairs can also be produced through other interactions such as the Higgs-fermion Yukawa interactions [Fig. 1(b)] in the Standard Model. These processes are collectively referred to as nonresonant production in this paper.

Higgs boson pair production at the LHC as a probe of the self-coupling has been extensively studied in the literature [9–13]. One conclusion [14] is that the data collected so far (approximately 25 fb^{-1} in total) are insensitive to the self-coupling in the SM, because of the expected small signal rates [15–17] and large backgrounds. However, it is essential to quantify the sensitivity of the current data set and to develop tools for future measurements. Moreover,

physics beyond the Standard Model (BSM) can potentially enhance the production rate and alter the event kinematics. For example, in the Minimal Supersymmetric Standard Model (MSSM) [18], a heavy CP-even neutral Higgs boson H can decay to a pair of lighter Higgs bosons. Production of H followed by its decay $H \to hh$ would lead to a new resonant process of Higgs boson pair production, in contrast to the nonresonant hh production predicted by the SM (Fig. 1). In composite Higgs models such as those discussed in Refs. [19,20], increased production of nonresonant Higgs boson pairs is also expected.

Both the ATLAS and CMS collaborations have searched for nonresonant and/or resonant Higgs boson pair production [21–23]. In particular, ATLAS has published the results of searches in the $hh \to \gamma\gamma bb$ [21] and $hh \to bbbb$ [22] decay channels.[1] In this paper, searches in two additional hh decay final states, $bb\tau\tau$ and $\gamma\gamma WW^*$, are reported. For the $hh \to bb\tau\tau$ analysis, one tau lepton is required to decay to an electron or a muon, collectively referred to as ℓ, and the other tau lepton decays to hadrons (τ_{had}). For $hh \to \gamma\gamma WW^*$, the $h \to WW^* \to \ell\nu qq'$ decay signature is considered in this study. The results of these new analyses are combined with the published results of $hh \to \gamma\gamma bb$ and $hh \to bbbb$ for both nonresonant and resonant production. The resonance mass m_H considered in this paper ranges from 260 to 1000 GeV. The lower bound is dictated by the $2m_h$ threshold while the upper bound is set by the search range of the $hh \to bb\tau\tau$ analysis. The light Higgs boson mass m_h is assumed to be 125.4 GeV, the central value of the ATLAS measurement [24]. At this mass value, the SM predictions [25–27] for the

---

[*]Full author list given at the end of the article.

[1]Notations indicating particle charges or antiparticles are generally omitted throughout this paper.
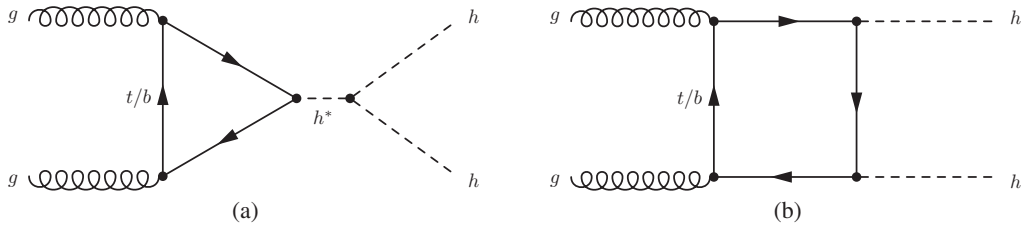
FIG. 1.   Leading-order Feynman diagrams of the nonresonant production of Higgs boson pairs in the Standard Model through (a) the Higgs boson self-coupling and (b) the Higgs-fermion Yukawa interactions only.

decay fractions of $hh \to bbbb$, $bb\tau\tau$, $bb\gamma\gamma$ and $\gamma\gamma WW^*$ are, respectively, 32.6%, 7.1%, 0.26%, and 0.10%. The resonant search assumes that gluon fusion is the production mechanism for a heavy Higgs boson that can subsequently decay to a pair of lighter Higgs bosons, i.e., $gg \to H \to hh$. Furthermore, the heavy Higgs boson is assumed to have a width significantly smaller than the detector resolution, which is approximately 1.5% in the best case (the $hh \to \gamma\gamma bb$ analysis). The potential interference between nonresonant and resonant production is ignored.

This paper is organized as follows. For the $hh \to bb\tau\tau$ and $hh \to \gamma\gamma WW^*$ analyses, data and Monte Carlo (MC) samples are described in Sec. II and the object reconstruction and identification are outlined in Sec. III. In Secs. IV and V, the separately published $hh \to \gamma\gamma bb$ and $hh \to bbbb$ analyses are briefly summarized. The $hh \to bb\tau\tau$ and $hh \to \gamma\gamma WW^*$ analyses including event selection, background estimations, and systematic uncertainties are presented in Secs. VI and VII, respectively. The statistical and combination procedure is described in Sec. VIII. The results of the $hh \to bb\tau\tau$ and $hh \to \gamma\gamma WW^*$ analyses, as well as their combinations with the published analyses are reported in Sec. IX. The implications of the resonant search

for two specific scenarios of the MSSM, hMSSM [28,29], and low-tb-high [30] are discussed in Sec. X. These scenarios make specific assumptions and/or choices of MSSM parameters to accommodate the observed Higgs boson. Finally, a summary is given in Sec. XI.

II. DATA AND MONTE CARLO SAMPLES

The data used in the searches were recorded in 2012 with the ATLAS detector at the Large Hadron Collider in proton-proton collisions at a center-of-mass energy of 8 TeV and correspond to an integrated luminosity of 20.3 fb^{-1}. The ATLAS detector is described in detail in Ref. [31]. Only data recorded when all subdetector systems were properly functional are used.

Signal and background MC samples are simulated with various event generators, each interfaced to Pythia v8.175 [32] for parton showers, hadronization and underlying-event simulation. Parton distribution functions (PDFs) CT10 [33] or CTEQ6L1 [34] for the proton are used depending on the generator in question. MSTW2008 [35] and NNPDF [36] PDFs are used to evaluate systematic uncertainties. Table I gives a brief overview of the event

TABLE I.   List of MC generators and parton distribution functions of the signal and background processes used by the $hh \to bb\tau\tau$ and $hh \to \gamma\gamma WW^*$ analyses. SM cross sections used for the normalization are also given. For the WZ and ZZ processes, contributions from γ^* are included and the cross sections quoted are for $m_{Z/\gamma^*} > 20$ GeV.

Process	Event generator	PDF set	Cross section [pb]
Background processes			
$V + \mathrm{jets}$	Alpgen+Pythia8	CTEQ6L1	normalized to data
Diboson: WW	Powheg+Pythia8	CT10	55.4
Diboson: WZ	Powheg+Pythia8	CT10	22.3
Diboson: ZZ	Powheg+Pythia8	CT10	7.3
$t\bar{t}$	Powheg+Pythia8	CT10	253
Single top: t-channel	AcerMC+Pythia8	CTEQ6L1	87.8
Single top: s-channel	Powheg+Pythia8	CT10	5.6
Single top: Wt	Powheg+Pythia8	CT10	22.0
$gg \to h$	Powheg+Pythia8	CT10	19.2
$q\bar{q}' \to q\bar{q}'h$	Powheg+Pythia8	CT10	1.6
$q\bar{q} \to Vh$	Pythia8	CTEQ6L1	1.1
$q\bar{q}/gg \to t\bar{t}h$	Pythia8	CTEQ6L1	0.13
Signal processes			
Nonresonant $gg \to hh$	MadGraph5+Pythia8	CTEQ6L1	0.0099
Resonant $gg \to H \to hh$	MadGraph5+Pythia8	CTEQ6L1	model dependent

generators, PDFs and cross sections used for the $hh \rightarrow bb\tau\tau$ and $hh \rightarrow \gamma\gamma WW^*$ analyses. All MC samples are passed through the ATLAS detector simulation program [37] based on GEANT4 [38].

Signal samples for both nonresonant and resonant Higgs boson pair production are generated using the leading-order MadGraph5 v1.5.14 [39] program. The non-resonant production is modeled using the SM DiHiggs model [40,41] while the resonant production is realized using the HeavyScalar model [42], both implemented in MadGraph5. The heavy scalar H is assumed to have a narrow decay width of 10 MeV, much smaller than the exper-imental resolution. The SM prediction for the nonresonant $gg \rightarrow hh$ production cross section is 9.9 ± 1.3 fb [17] with $m_h = 125.4$ GeV from the next-to-next-to-leading-order calculation in QCD.

Single SM Higgs boson production is considered as a background. The Powheg r1655 generator [43–45] is used to produce gluon fusion (ggF) and vector-boson fusion (VBF) events. This generator calculates QCD corrections up to next-to-leading order (NLO), including finite bottom- and top-quark mass effects [46]. The Higgs boson transverse momentum (p_T) spectrum of the ggF process is matched to the calculated spectrum at next-to-next-to-leading order (NNLO) and next-to-next-to-leading logarithm (NNLL) [47] in QCD corrections. Events of associated production $q\bar{q} \rightarrow Vh$ (here $V = W$ or Z) and $q\bar{q}/gg \rightarrow t\bar{t}h$ are produced using the Pythia8 generator [32]. All of these backgrounds are normalized using the state-of-the-art theoretical cross sections (see Table I) and their uncertain-ties compiled in Refs. [25–27].

The Alpgen v2.1.4 program [48] is used to produce the V + jets samples. The Powheg generator is used to simulate top quark pair production ($t\bar{t}$) as well as the s-channel and Wt processes of single top production; the t-channel process of single top production is simulated using the AcerMC v38 program [49]. The $t\bar{t}$ cross section has been calculated up to NNLO and NNLL in QCD corrections [50]. Cross sections for the three single-top processes have been calculated at (approximate) NNLO accuracy [51–53]. The Powheg generator is used to simulate diboson back-grounds (WW, WZ, and ZZ). The diboson production cross sections are calculated at NLO in QCD corrections using the MCFM program [54,55].

III. OBJECT IDENTIFICATION

In this section, object reconstruction and identification for the $hh \rightarrow bb\tau\tau$ and $hh \rightarrow \gamma\gamma WW^*$ analyses are dis-cussed. The $hh \rightarrow bb\tau\tau$ and $hh \rightarrow \gamma\gamma WW^*$ analyses are developed following the $h \rightarrow \tau\tau$ [6] and $h \rightarrow \gamma\gamma$ [56] studies of single Higgs bosons, respectively, and use much of their methodology.

Electrons are reconstructed from energy clusters in the electromagnetic calorimeter matched to tracks in the inner tracker. The calorimeter shower profiles of electron

candidates must be consistent with those expected from electromagnetic interactions. Electron candidates are iden-tified using tight and medium criteria [57] for the $hh \rightarrow bb\tau\tau$ and $hh \rightarrow \gamma\gamma WW^*$ analyses, respectively. The selec-ted candidates are required to have transverse momenta[2] $p_T > 15$ GeV and be within the detector fiducial volume of $|\eta| < 2.47$ excluding $1.37 < |\eta| < 1.52$, the transition region between the barrel and endcap calorimeters. Muons are identified by matching tracks or segments reconstructed in the muon spectrometer with tracks reconstructed in the inner tracker. They are required to have $p_T > 10$ GeV and $|\eta| < 2.5$. Both the electrons and muons must satisfy calorimeter and track isolation requirements. The calorim-eter isolation requires that the energy deposited in the calorimeter in a cone of size $\Delta R \equiv \sqrt{(\Delta\eta)^2 + (\Delta\phi)^2} = 0.2$ around the lepton (electron or muon), excluding the energy deposited by the lepton itself, is less than 6% (20%) of the p_T of the lepton for the $hh \rightarrow bb\tau\tau$ ($hh \rightarrow \gamma\gamma WW^*$) analysis. The track isolation is defined similarly: the scalar p_T sum of additional tracks originating from the primary vertex with $p_T > 1$ GeV in a cone of size $\Delta R = 0.4$ around the lepton is required to be less than 6% (15%) of the p_T of the lepton track for the $hh \rightarrow bb\tau\tau$ ($hh \rightarrow \gamma\gamma WW^*$) analysis.

Photons are reconstructed from energy clusters in the electromagnetic calorimeter with their shower profiles consistent with electromagnetic showers. A significant fraction of photons convert into e^+e^- pairs inside the inner tracker. Thus photon candidates are divided into uncon-verted and converted categories. Clusters without matching tracks are considered as unconverted photons, while clusters matched to tracks consistent with conversions are considered as converted photons. Photon candidates must fulfill the tight identification criteria [58] and are required to have $p_T > 25$ GeV and $|\eta| < 2.37$ (excluding the transition region $1.37 < |\eta| < 1.52$) and must satisfy both calorimeter and track isolation. The calorimeter isolation requires the additional energy in a cone of $\Delta R = 0.4$ around the photon candidate to be less than 6 GeV while the track isolation requires the scalar p_T sum of additional tracks in a cone of $\Delta R = 0.2$ around the photon to be less than 2.6 GeV.

Jets are reconstructed using the anti-k_t algorithm [59] with a radius parameter of $R = 0.4$. Their energies are corrected for the average contributions from pileup inter-actions. Jets are required to have $p_T > 30$ GeV and $|\eta| < 4.5$. For the $hh \rightarrow \gamma\gamma WW^*$ analysis, a lower p_T requirement of 25 GeV is applied for jets in the central region of $|\eta| < 2.4$. To suppress contributions from pileup interactions, jets with $p_T < 50$ GeV and within

---

[2]ATLAS uses a right-hand coordinate system with the inter-action point as its origin and the beam line as its z axis. The x axis points to the center of the LHC ring and y axis points upwards. The pseudorapidity η is defined as $\eta = -\ln\tan(\theta/2)$, where θ is the polar angle measured with respect to the z axis. The transverse momentum p_T is calculated from the momentum p: $p_T = p\sin\theta$.

the acceptance of the inner tracker ($|\eta| < 2.4$) must have over 50% of the scalar sum of the p_T of their associated tracks contributed by those originating from the primary vertex. Jets containing b-hadrons are identified using a multivariate algorithm (b-tagging) [60]. The algorithm combines information such as the explicit reconstruction of the secondary decay vertices and track impact-parameter significances. The operating point chosen for both $hh \rightarrow bb\tau\tau$ and $hh \rightarrow \gamma\gamma WW^*$ analyses has an efficiency of 80% for the b-quark jets in $t\bar{t}$ events.

Hadronically decaying τ candidates (τ_{had}) are reconstructed using clusters in the electromagnetic and hadronic calorimeters [61]. The tau candidates are required to have $p_T > 20$ GeV and $|\eta| < 2.5$. The number of tracks with $p_T > 1$ GeV associated with the candidates must be one or three and the total charge determined from these tracks must be ± 1. The tau identification uses calorimeter cluster as well as tracking-based variables, combined using a boosted-decision-tree method [61]. Three working points, labeled loose, medium, and tight [61], corresponding to different identification efficiencies are used. Dedicated algorithms that suppress electrons and muons misidentified as τ_{had} candidates are applied as well.

The missing transverse momentum (with magnitude E_T^{miss}) is the negative of the vector sum of the transverse momenta of all photon, electron, muon, τ_{had}, and jet candidates, as well as the p_T of all calorimeter clusters not associated with these reconstructed objects, called the soft-term contribution [62]. The $hh \rightarrow bb\tau\tau$ analysis uses the version of the E_T^{miss} calculation in the $h \rightarrow \tau\tau$ analysis [6]. In this calculation, the soft-term contribution is scaled by a vertex fraction, defined as the ratio of the summed scalar p_T of all tracks from the primary vertex not matched with the reconstructed objects to the summed scalar p_T of all tracks in the event. The $hh \rightarrow \gamma\gamma WW^*$ analysis, on the other hand, uses the E_T^{miss}-significance employed by the $h \rightarrow \gamma\gamma$ study [56]. It is defined as the ratio of the measured E_T^{miss} to its expected resolution estimated using the square root of the scalar sum of the transverse energies of all objects contributing to the E_T^{miss} calculation.

IV. SUMMARY OF $hh \rightarrow \gamma\gamma bb$

The $hh \rightarrow \gamma\gamma bb$ analysis, published in Ref. [21], largely follows the ATLAS analysis of the Higgs boson discovery in the $h \rightarrow \gamma\gamma$ decay channel [1,56]. The search is performed in the $\sqrt{s} = 8$ TeV data set corresponding to an integrated luminosity of 20.3 fb^{-1}. The data were recorded with diphoton triggers that are nearly 100% efficient for events satisfying the photon requirements. Events must contain two isolated photons. The p_T for the leading (subleading) photon must be larger than 35% (25%) of the diphoton invariant mass $m_{\gamma\gamma}$, which itself must be in the range of $105 < m_{\gamma\gamma} < 160$ GeV. Events must also contain two energetic b-tagged jets; the leading (subleading) jet must have $p_T > 55$ (35) GeV, and the dijet mass must fall

within a window $95 < m_{bb} < 135$ GeV, as expected from the $h \rightarrow bb$ decay. A multivariate b-tagging algorithm [60] that is 70% efficient for the b-quark jets in $t\bar{t}$ events is applied.

Backgrounds for both the resonant and nonresonant analyses are divided into two categories: events containing a single real Higgs boson (with $h \rightarrow \gamma\gamma$), and the continuum background of events not containing a Higgs boson. The former are evaluated purely from simulation, and are small compared to the continuum background, which is evaluated from data in the diphoton mass sidebands (the $m_{\gamma\gamma}$ range of 105–160 GeV excluding the region of $m_h \pm 5$ GeV). In the nonresonant analysis, an unbinned signal-plus-background fit is performed on the observed $m_{\gamma\gamma}$ distribution, with the background from single Higgs bosons constrained to the expectation from the SM. The continuum background is modeled with an exponential function; the shape of the exponential function is taken from data containing a diphoton and dijet pair where fewer than two jets are b-tagged.

The resonant search proceeds in a similar manner, although it is ultimately a counting experiment, with an additional requirement on the four-object invariant mass $m_{\gamma\gamma bb}$, calculated with the bb mass constrained to m_h. This requirement on $m_{\gamma\gamma bb}$ varies with the resonance mass hypothesis under evaluation, and is defined as the smallest window containing 95% of the signal events based on MC simulation. As in the nonresonant search, the number of background events with real Higgs bosons is estimated from simulation. The continuum background in the $m_{\gamma\gamma}$ signal window is extrapolated from the diphoton mass sidebands. A resonance with mass between 260 and 500 GeV is considered in the search.

The small number of events (nine) in the diphoton mass sideband leads to large statistical uncertainties (33%) on the dominant continuum background, so that most systematic uncertainties have a small effect on the final result. For the resonant search, however, systematic uncertainties with comparable effect remain. Uncertainties of 0%–30% (depending on the resonance mass hypothesis under consideration) are assigned due to the modeling of the $m_{\gamma\gamma bb}$ shape using the data with less than two b-tagged jets. Additional uncertainties of 16%–30% arise from the choice of functional form used to parametrize the shape of $m_{\gamma\gamma bb}$.

In the nonresonant analysis, extrapolating the sidebands into the diphoton mass window of the signal selection leads to a prediction of 1.3 continuum background events. An additional contribution of 0.2 events is predicted from single Higgs boson production. A total of five events are observed, representing an excess of 2.4 standard deviations (σ). A 95% confidence level (C.L.) upper limit of 2.2 (1.0) pb is observed (expected) for $\sigma(gg \rightarrow hh)$, the cross section of nonresonant Higgs boson pair production. For the resonant searches, the observed (expected) upper limits

on $\sigma(gg \to H) \times \mathrm{BR}(H \to hh)$ are 2.3 (1.7) pb at $m_H = 260$ GeV and 0.7 (0.7) pb at $m_H = 500$ GeV.

V. SUMMARY OF $hh \to bbbb$

The $hh \to bbbb$ analysis [22] benefits from the large branching ratio of $h \to bb$. The analysis employs resolved as well as boosted Higgs boson reconstruction methods. The resolved method attempts to reconstruct and identify separate b-quark jets from the $h \to bb$ decay, while the boosted method uses a jet substructure technique to identify the $h \to bb$ decay reconstructed as a single jet. The latter is expected if the Higgs boson h has a high momentum. The boosted method is particularly suited to the search for a resonance with mass above approximately 1000 GeV decaying to a pair of SM Higgs bosons. For the combinations presented in this paper, resonances below this mass are considered and the resolved method is used as it is more sensitive.

The analysis with the resolved method searches for two back-to-back and high-momentum bb systems with their masses consistent with m_h in a data set at $\sqrt{s} = 8$ TeV corresponding to an integrated luminosity of 19.5 fb^{-1} for the triggers used. The data were recorded with a combination of multijet triggers using information including the b-quark jet tagging. The trigger is $> 99.5\%$ efficient for signal events satisfying the offline selection. Candidate events are required to have at least four b-tagged jets, each with $p_T > 40$ GeV. As in the $hh \to \gamma\gamma bb$ analysis, a multivariate b-tagging algorithm [60] with an estimated efficiency of 70% is used to tag jets containing b-hadrons. The four highest-p_T b-tagged jets are then used to form two dijet systems, requiring the angular separation ΔR in (η, ϕ) space between the two jets in each of the two dijet systems to be smaller than 1.5. The transverse momenta of the leading and subleading dijet systems must be greater than 200 and 150 GeV, respectively. These selection criteria, driven partly by the corresponding jet trigger thresholds and partly by the necessity to suppress the backgrounds, lead to significant loss of signal acceptance for lower resonance masses. The resonant search only considers masses above 500 GeV. The leading (m_{12}) and subleading (m_{34}) dijet invariant mass values are required to be consistent with those expected for the $hh \to bbbb$ decay, satisfying the requirement:

$$\sqrt{\left(\frac{m_{12} - m_{12}^0}{\sigma_{12}}\right)^2 + \left(\frac{m_{34} - m_{34}^0}{\sigma_{34}}\right)^2} < 1.6.$$

Here m_{12}^0 (124 GeV) and m_{34}^0 (115 GeV) are the expected peak values from simulation for the leading and subleading dijet pair, respectively, and σ_{12} and σ_{34} are the dijet mass resolutions, estimated from the simulation to be 10% of the dijet mass values. More details about the selection can be found in Ref. [22].

After the full selection, more than 90% of the total background in the signal region is estimated to be multijet events, while the rest is mostly $t\bar{t}$ events. The $Z + \text{jets}$ background constitutes less than 1% of the total background and is modeled using MC simulation. The multijet background is modeled using a fully data-driven approach in an independent control sample passing the same selection as the signal except that only one of the two selected dijets is b-tagged. This control sample is corrected for the kinematic differences arising from the additional b-tagging requirements in the signal sample. The $t\bar{t}$ contribution is taken from MC simulations normalized to data in dedicated control samples.

The dominant sources of systematic uncertainty in the analysis are the b-tagging calibration and the modeling of the multijet background. The degradation in the analysis sensitivity from these uncertainties is below 10%. Other sources of systematic uncertainty include the $t\bar{t}$ modeling, and the jet energy scale and resolution, which are all at the percent level. A total of 87 events are observed in the data, in good agreement with the SM expectation of 87.0 ± 5.6 events. Good agreement is also observed in the four-jet invariant mass distribution, thus there is no evidence of Higgs boson pair production. For the nonresonant search, both the observed and expected 95% C.L. upper limit on the cross section $\sigma(pp \to hh \to bbbb)$ is 202 fb. For the resonant search, the invariant mass of the four jets is used as the final discriminant from which the upper limit on the potential signal cross section is extracted. The resulting observed (expected) 95% C.L. upper limit on $\sigma(pp \to H \to hh \to bbbb)$ ranges from 52 (56) fb, at $m_H = 500$ GeV, to 3.6 (5.8) fb, at $m_H = 1000$ GeV.

VI. $hh \to bb\tau\tau$

This section describes the search for Higgs boson pair production in the $hh \to bb\tau\tau$ decay channel, where only the final state where one tau lepton decays hadronically and the other decays leptonically, $bb\ell\tau_{\mathrm{had}}$, is used. The data were recorded with triggers requiring at least one lepton with $p_T > 24$ GeV. These triggers are nearly 100% efficient for events passing the final selection. Candidate $bb\ell\tau_{\mathrm{had}}$ events are selected by requiring exactly one lepton with $p_T > 26$ GeV, one hadronically decaying tau lepton of the opposite charge with $p_T > 20$ GeV meeting the medium criteria [61], and two or more jets with $p_T > 30$ GeV. In addition, between one and three of the selected jets must be b-tagged using the multivariate b-tagger. The upper bound on the number of b-tagged jets is designed to make this analysis statistically independent of the $hh \to bbbb$ analysis summarized in Sec. V. These criteria are collectively referred to as the "preselection".

The backgrounds from $W + \text{jets}$, $Z \to \tau\tau$, diboson (WW, WZ, and ZZ), and top quark (both $t\bar{t}$ and single top quark) production dominate the surviving sample and their contributions are derived from a mixture of data-driven

methods and simulation. The contribution from events with a jet misidentified as a τ_{had}, referred to as the fake τ_{had} background, are estimated using data with a "fake-factor" method. The method estimates contributions from $W+$jets, multijet, $Z+$jets, and top quark events that pass the event selection due to misidentified τ_{had} candidates. The fake factor is defined as the ratio of the number of τ_{had} candidates identified as medium, to the number satisfying the loose, but not the medium, criteria [61]. The p_{T}-dependent fake factors are measured in data control samples separately for the τ_{had} candidates with one or three tracks and for $W+$jets, multijet, $Z+$jets, and top quark contributions. The $W+$jets, multijet, $Z+$jets, and top quark control samples are selected by reversing the m_{T} cut (see below), relaxing the lepton isolation requirement, reversing the dilepton veto or by requiring b-tagged jets, respectively. The fake factors determined from these control samples are consistent within their statistical uncertainties. They are then applied to the signal control sample, i.e., events passing the selection, except that the τ_{had} candidate is required to satisfy the loose, but not the medium, τ_{had} identification, to estimate the fake τ_{had} background. The composition of the sample is determined from a mixture of data-driven methods and MC simulations and it is found that the sample is dominated by the $W+$jets and multijet events. Details of the method can be found in Ref. [61]. The method is validated using the same-sign $\ell\tau_{\text{had}}$ events that are otherwise selected in the same way as the signal candidates.

The $Z \to \tau\tau$ background is modeled using selected $Z \to \mu\mu$ events in data through embedding [63], where the muon tracks and associated energy depositions in the calorimeters are replaced by the corresponding simulated signatures of the final-state particles of tau decays. In this approach, the kinematics of the produced boson, the hadronic activity of the event (jets and underlying event) as well as pileup are taken from data [6]. Other processes passing the $Z \to \mu\mu$ selection, primarily from top quark production, are subtracted from the embedded data sample using simulation. Their contributions are approximately 2% for events with one b-tagged jet and 25% for events with two or more b-tagged jets. The $Z \to \tau\tau$ background derived is found to be in a good agreement with that obtained from the MC simulation.

The remaining backgrounds, mostly $t\bar{t}$ and diboson events with genuine $\ell\tau_{\text{had}}$ in their decay final states, are estimated using simulation. The small contributions from single SM Higgs boson production and from $Z(\to ee/\mu\mu)+$jets events (in which one of the electrons or muons is misidentified as τ_{had}) are also estimated from simulation. The production rates of these processes are normalized to the theoretical cross sections discussed in Sec. II. For the simulation of the $t\bar{t}$ process, the top quark p_{T} distribution is corrected for the observed difference between data and simulation [64]. The background from misidentified leptons is found to be negligible.

Figures 2(a) and 2(b) compare the observed ditau ($m_{\tau\tau}$) and dijet (m_{bb}) mass distributions with those expected from background events after the preselection discussed above. The sample is dominated by contributions from top quark production, fake τ_{had}, and $Z \to \tau\tau$ backgrounds. Also shown in the figures are the expected signal distributions for a Higgs boson pair production cross section of 20 pb as an illustration. The yield of the nonresonant production is significantly higher than that of the resonant production for the same cross section, largely due to the harder p_{T} spectrum of the Higgs boson h of the nonresonant production. The ditau invariant mass is reconstructed from the electron or muon, τ_{had}, and $E_{\text{T}}^{\text{miss}}$ using a method known as the missing mass calculator (MMC) [65]. The MMC solves an underconstrained system of equations with solutions weighted by $E_{\text{T}}^{\text{miss}}$ resolution and the tau-lepton decay topologies. It returns the most probable value of the ditau mass, assuming that the observed lepton, τ_{had} and $E_{\text{T}}^{\text{miss}}$ stem from a $\tau\tau$ resonance. The dijet mass is calculated from the two leading b-tagged jets, or using also the highest-p_{T} untagged jet if only one jet is b-tagged.

Additional topological requirements are applied to reduce the background. As shown in Fig. 2(c), the signal events tend to have small values of the transverse mass $m_{\text{T}}^{\ell\nu}$ calculated from the lepton and $E_{\text{T}}^{\text{miss}}$ system. Consequently, a requirement of $m_{\text{T}}^{\ell\nu} < 60$ GeV is applied, which reduces the background significantly with only a small loss of the signal efficiency. In addition, the angular separation in the transverse plane between the $E_{\text{T}}^{\text{miss}}$ and τ_{had} is required to be larger than one radian to reduce the fake τ_{had} background.

Background events from $t\bar{t} \to WWbb \to \ell\nu\tau\nu bb$ decay have an identical visible final state to the signal if the tau lepton decays hadronically. For signal $h \to \tau\tau \to \ell\tau_{\text{had}}$ events, however, the p_{T} of the lepton tends to be softer than that of the τ_{had} due to the presence of more neutrinos in the $\tau \to \ell$ decays. Thus the p_{T} of the electron or muon is required to satisfy $p_{\text{T}}(\ell) < p_{\text{T}}(\tau_{\text{had}}) + 20$ GeV. The $t\bar{t}$ events of the $t\bar{t} \to WWbb \to \ell\nu qq'bb$ final state with a misidentified τ_{had} candidate remain a large background. To reduce its contribution, a W boson candidate is reconstructed from the τ_{had} candidate and its closest untagged jet and its mass $m_{\tau j}$ is calculated. The W candidate is then paired with a b-tagged jet to form the top quark candidate with a reconstructed mass $m_{\tau jb}$. The pairing is chosen to minimize the mass sum $m_{\ell b} + m_{\tau b}$ for events with two or more b-tagged jets. If only one jet is b-tagged, one of the b-jets in the mass sum is replaced by the highest-p_{T} untagged jet. An elliptical requirement in the form of a χ^2 in the $(m_{\tau j}, m_{\tau jb})$ plane:

$$\left(\frac{\Delta m_W \cos\theta - \Delta m_t \sin\theta}{28\,\text{GeV}}\right)^2 + \left(\frac{\Delta m_W \sin\theta + \Delta m_t \cos\theta}{18\,\text{GeV}}\right)^2 > 1$$

is applied to reject events with $(m_{\tau j}, m_{\tau jb})$ consistent with the hypothesis (m_W, m_t), the masses of the W boson and
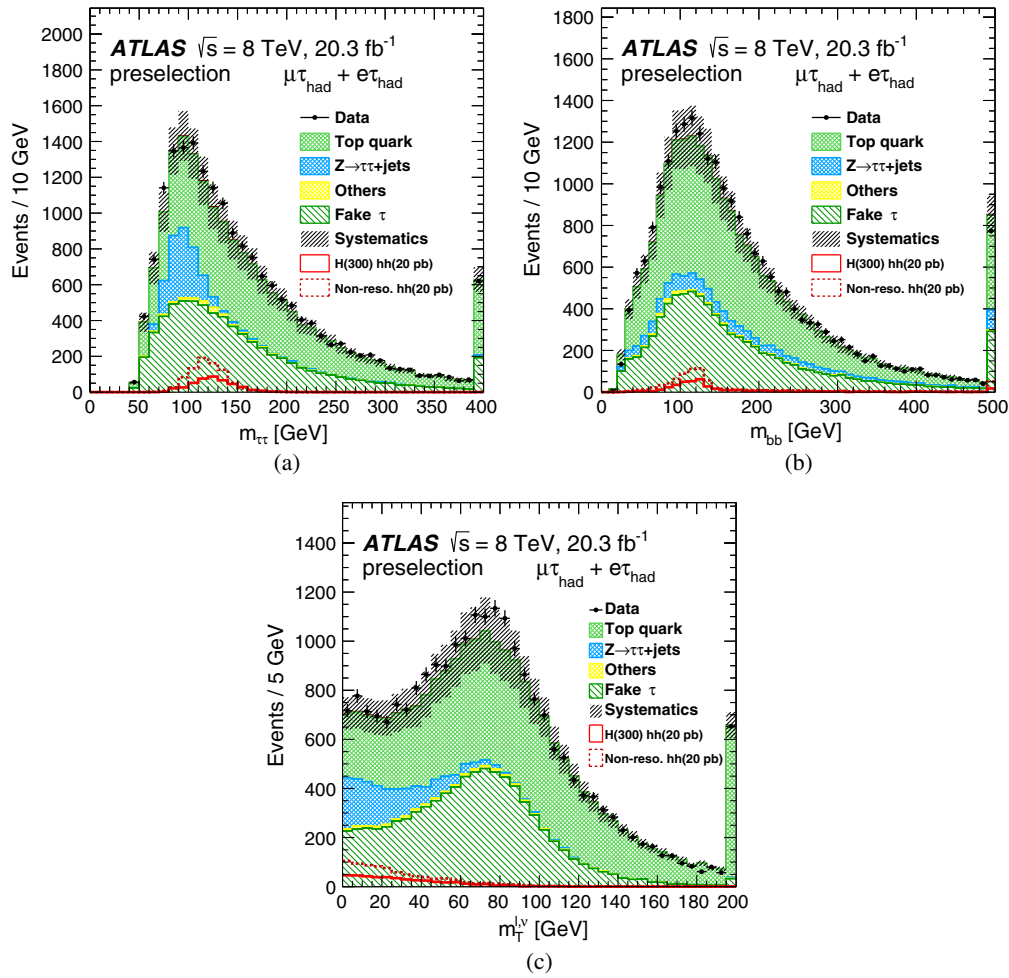
FIG. 2 (color online). Kinematic distributions of the $hh \to bb\tau\tau$ analysis after the preselection (see text) comparing data with the expected background contributions: (a) ditau mass $m_{\tau\tau}$ reconstructed using the MMC method, (b) dijet mass m_{bb}, and (c) the transverse mass $m_T^{\ell\nu}$ of the lepton and the E_T^{miss} system. The top quark background includes contributions from both $t\bar{t}$ and the single top-quark production. The background category labeled "Others" comprises diboson and $Z \to ee/\mu\mu$ contributions. Contributions from single SM Higgs boson production are included in the background estimates, but are too small to be visible on these distributions. As illustrations, expected signal distributions for a Higgs boson pair production cross section of 20 pb are overlaid for both nonresonant and resonant Higgs boson pair production. A mass of $m_H = 300$ GeV is assumed for the resonant production. The last bin in all distributions represents overflows. The gray hatched bands represent the uncertainties on the total background contributions. These uncertainties are largely correlated from bin to bin.

the top quark. Here $\Delta m_W = m_{\tau j} - m_W$, $\Delta m_t = m_{\tau jb} - m_t$ and θ is a rotation angle given by $\tan\theta = m_t/m_W$ to take into account the average correlation between $m_{\tau j}$ and $m_{\tau jb}$.

Finally, the remaining events must have $90 < m_{bb} < 160$ GeV, consistent with the expectation for the $h \to bb$ decay. For the nonresonant search, $m_{\tau\tau}$ is used as the final discriminant to extract the signal, and its distribution is shown in Fig. 3(a). The selection efficiency for the $gg \to hh \to bb\tau\tau$ signal is 0.57%. For the resonant search, the MMC mass is required to be in the range of $100 < m_{\tau\tau} < 150$ GeV. The mass resolutions of m_{bb} and $m_{\tau\tau}$ are comparable for the signal, but the m_{bb} distribution has a longer tail. The resonance mass $m_{bb\tau\tau}$ reconstructed from

the dijet and ditau system is used as the discriminant. To improve the mass resolution of the heavy resonances, scale factors of m_h/m_{bb} and $m_h/m_{\tau\tau}$ are applied respectively to the four-momenta of the bb and $\tau\tau$ systems, where m_h is set to the value of 125 GeV used in the simulation. The resolution of $m_{bb\tau\tau}$ is found from simulation studies to vary from 2.4% at $m_H = 260$ GeV to 4.8% at 1000 GeV. The improvement in the resolution from the rescaling is largest at low mass and varies from approximately a factor of 3 at 260 GeV to about 30% at 1000 GeV. The reconstructed $m_{bb\tau\tau}$ distribution for events passing all the selections is shown in Fig. 3(b). The efficiency for the $gg \to H \to hh \to bb\tau\tau$ signal varies from 0.20% at 260 GeV to 1.5% at 1000 GeV. These efficiencies include branching ratios of
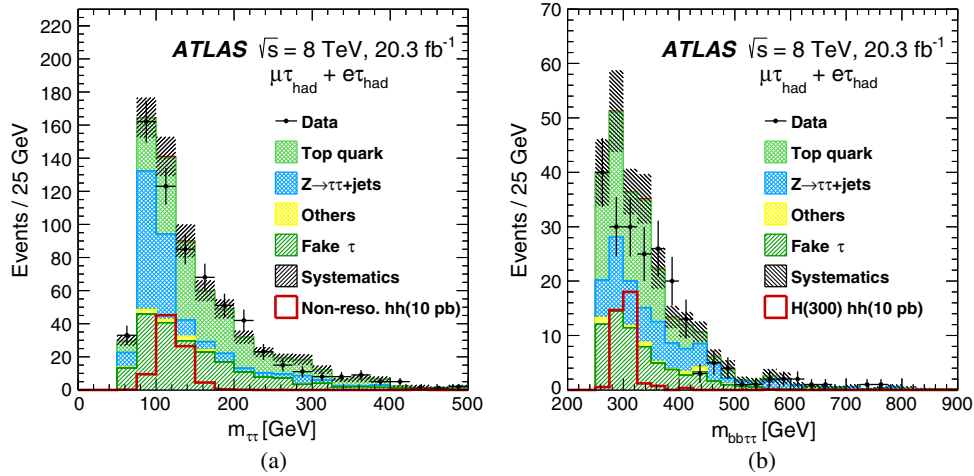
FIG. 3 (color online).   Distributions of the final discriminants used to extract the signal: (a) $m_{\tau\tau}$ for the nonresonant search and (b) $m_{bb\tau\tau}$ for the resonant search. The top quark background includes contributions from both $t\bar{t}$ and the single top-quark production. The background category labeled "Others" comprises diboson and $Z \to ee/\mu\mu$ contributions. Contributions from single SM Higgs boson production are included in the background estimates, but are too small to be visible on these distributions. As illustrations, the expected signal distributions assume a cross section of 10 pb for Higgs boson pair production for both the nonresonant and resonant searches. In (b), a resonance mass of 300 GeV is assumed. The gray hatched bands represent the uncertainties on the total backgrounds. These uncertainties are largely correlated from bin to bin.

the tau lepton decays, but not those of heavy or light Higgs bosons.

To take advantage of different signal-to-background ratios in different kinematic regions, the selected events are divided into four categories based on the ditau transverse momentum $p_T^{\tau\tau}$ (less than or greater than 100 GeV) and the number of b-tagged jets ($n_b = 1$ or ≥ 2) for both the nonresonant and resonant searches. The numbers of events expected from background processes and observed in the data passing the resonant $hh \to bb\tau\tau$ selection are summarized in Table II for each of the four categories. The expected number of events from the production of a Higgs boson with $m_H = 300$ GeV and a cross section of $\sigma(gg \to H) \times \mathrm{BR}(H \to hh) = 1$ pb for each category is also shown for comparison.

Systematic uncertainties from the trigger, luminosity, object identification, background estimate as well as Monte Carlo modeling of signal and background processes are taken into account in the background estimates and the calculation of signal yields. The impact of these systematic uncertainties varies for different background components and event categories. For the most sensitive $n_b \geq 2$ categories, the main background contributions are from top quark, fake τ_{had}, and $Z \to \tau\tau$. The jet energy scale and resolution is the largest uncertainty for the top-quark contribution, ranging between 10% and 19% for the nonresonant and resonant searches. The leading source of systematic uncertainty for the fake τ_{had} background is the "fake-factor" determination, due to the uncertainties of the sample composition. Varying the composition of W + jets,

TABLE II.   The numbers of events predicted from background processes and observed in the data passing the final selection of the resonant search for the four categories. The top quark background includes contributions from both $t\bar{t}$ and the single top-quark production. The "others" background comprises diboson and $Z \to ee/\mu\mu$ contributions. The numbers of events expected from the production of a $m_H = 300$ GeV Higgs boson with a cross section of $\sigma(gg \to H) \times \mathrm{BR}(H \to hh) = 1$ pb are also shown as illustrations. The uncertainties shown are the total uncertainties, combining statistical and systematic components.

	$n_b = 1$		$n_b \geq 2$	
Process	$p_T^{\tau\tau} < 100$ GeV	$p_T^{\tau\tau} > 100$ GeV	$p_T^{\tau\tau} < 100$ GeV	$p_T^{\tau\tau} > 100$ GeV
SM Higgs	0.5 ± 0.1	0.8 ± 0.1	0.1 ± 0.1	0.2 ± 0.1
Top quark	30.3 ± 3.6	19.6 ± 2.5	30.9 ± 3.0	23.6 ± 2.5
$Z \to \tau\tau$	38.1 ± 4.4	20.2 ± 3.7	6.8 ± 1.8	2.6 ± 1.0
Fake τ_{had}	37.0 ± 4.4	12.1 ± 1.7	13.7 ± 1.9	5.4 ± 1.0
Others	3.2 ± 3.7	0.5 ± 1.5	0.7 ± 1.6	0.2 ± 0.7
Total background	109.1 ± 8.6	53.1 ± 6.0	52.2 ± 8.2	32.1 ± 5.4
Data	92	46	35	35
Signal $m_H = 300$ GeV	0.8 ± 0.2	0.4 ± 0.2	1.5 ± 0.3	0.9 ± 0.2

Z + jets, top quark and multijet events in the control samples by $\pm50\%$ leads to a change in the estimated fake τ_{had} background by 9.5%. The most important source of systematic uncertainty for the $Z \to \tau\tau$ background is the $t\bar{t}$ subtraction from the $Z \to \mu\mu$ sample used for the embedding, due to the uncertainty on the $t\bar{t}$ normalization. Its effect ranges from 8% to 15%. The overall systematic uncertainties on the total background contributions to the high (low) $p_{\mathrm{T}}^{\tau\tau}$ category of $n_b \geq 2$ are 12% (9%) for the nonresonant search and 14% (14%) for the resonant search. The largest contributions are from jet and tau energy scales and b-tagging. The modeling of top quark production is also an important systematic uncertainty for the category with two or more b-tagged jets and high $p_{\mathrm{T}}^{\tau\tau}$.

The uncertainties on the signal acceptances are estimated from experimental as well as theoretical sources. The total experimental systematic uncertainties vary between 12% and 24% for the categories with two or more b-tagged jets, and are dominated by the jet and tau energy scales and b-tagging. Theoretical uncertainties arise from the choice of parton distribution functions, the renormalization and factorization scales as well as the value of strong coupling constant α_s used to generate the signal events. Uncertainties of 3%, 1%, and 3% from the three sources, respectively, are assigned to all signal acceptances.

For the nonresonant search, the observed ditau mass distribution agrees well with that of the estimated background events as shown in Fig. 3(a). For the resonant search, a small deficit with a local significance of approximately 2σ is observed in the data relative to the background expectation at $m_{bb\tau\tau} \sim 300$ GeV as is shown in Fig. 3(b). No evidence of Higgs boson pair production is present in the data. The resulting upper limits on Higgs boson pair production from these searches are described in Sec. IX.

VII. $hh \to \gamma\gamma WW^*$

This section describes the search for Higgs boson pair production in the $hh \to \gamma\gamma WW^*$ decay channel, where one Higgs boson decays to a pair of photons and the other decays to a pair of W bosons. The $h \to \gamma\gamma$ decay is well suited for tagging the Higgs boson. The small Higgs boson width together with the excellent detector resolution for the diphoton mass strongly suppresses background contributions. Moreover, the $h \to WW^*$ decay has the largest branching ratio after $h \to bb$. To reduce multijet backgrounds, one of the W bosons is required to decay to an electron or a muon (either directly or through a tau lepton) whereas the other is required to decay hadronically, leading to the $\gamma\gamma\ell\nu qq'$ final state.

The data used in this analysis were recorded with diphoton triggers with an efficiency close to 100% for diphoton events passing the final offline selection. The diphoton selection follows closely that of the ATLAS measurement of the $h \to \gamma\gamma$ production rate [56] and that of

the $hh \to \gamma\gamma bb$ analysis [21]. Events are required to have two or more identified photons with the leading and subleading photon candidates having $p_{\mathrm{T}}/m_{\gamma\gamma} > 0.35$ and 0.25, respectively, where $m_{\gamma\gamma}$ is the invariant mass of the two selected photons. Only events with $m_{\gamma\gamma}$ in the range of $105 < m_{\gamma\gamma} < 160$ GeV are considered.

Additional requirements are applied to identify the $h \to WW^* \to \ell\nu qq'$ decay signature. Events must have two or more jets, and exactly one lepton, satisfying the identification criteria described in Sec. III. To reduce multijet backgrounds, the events are required to have $E_{\mathrm{T}}^{\mathrm{miss}}$ with significance greater than one. Events with any b-tagged jet are vetoed to reduce contributions from top quark production.

A total of 13 events pass the above selection. The final $hh \to \gamma\gamma WW^*$ candidates are selected by requiring the diphoton mass $m_{\gamma\gamma}$ to be within a $\pm2\sigma$ window of the Higgs boson mass in $h \to \gamma\gamma$ where σ is taken to be 1.7 GeV. Due to the small number of events, both nonresonant and resonant searches proceed as counting experiments. The selection efficiency for the $hh \to \gamma\gamma WW^*$ signal of SM nonresonant Higgs boson pair production is estimated using simulation to be 2.9%. For the resonant production, the corresponding efficiency varies from 1.7% at 260 GeV to 3.3% at 500 GeV. These efficiencies include the branching ratios of the W boson decays, but not those of the Higgs boson decays.

The background contributions considered are single SM Higgs boson production (gluon fusion, vector-boson fusion, and associated production of Wh, Zh, and $t\bar{t}h$) and continuum backgrounds in the $m_{\gamma\gamma}$ spectrum. Events from single Higgs boson production can mimic the $hh \to \gamma\gamma WW^*$ signal if, for example, the Higgs boson decays to two photons and the rest of the event satisfies the $h \to WW^* \to \ell\nu qq'$ identification. These events would exhibit a diphoton mass peak at m_h. As in the $hh \to bb\tau\tau$ analysis, their contributions are estimated from simulation using the SM cross sections [27]. The systematic uncertainty on the total yield of these backgrounds is estimated to be 29%, dominated by the modeling of jet production (27%). The total number of events expected from single SM Higgs production is therefore 0.25 ± 0.07 with contributions of 0.14, 0.08, and 0.025 events from Wh, $t\bar{t}h$, and Zh processes, respectively. Contributions from gluon and vector-boson fusion processes are negligible.

The background that is nonresonant in the $\gamma\gamma$ mass spectrum is measured using the continuum background in the $m_{\gamma\gamma}$ spectrum. The major source of these backgrounds is $W\gamma\gamma$ + jets events with a $W \to \ell\nu$ decay. These events are expected to have a diphoton mass distribution with no resonant structure at m_h and their contribution ($N_{\mathrm{SR}}^{\mathrm{est}}$) in the signal region, $m_{\gamma\gamma} \in m_h \pm 2\sigma$, is estimated from the $m_{\gamma\gamma}$ sidebands in the data:

$$N_{\mathrm{SR}}^{\mathrm{est}} = N_{\mathrm{SB}}^{\mathrm{Data}} \times \frac{f_{\mathrm{SB}}}{1 - f_{\mathrm{SB}}}.$$
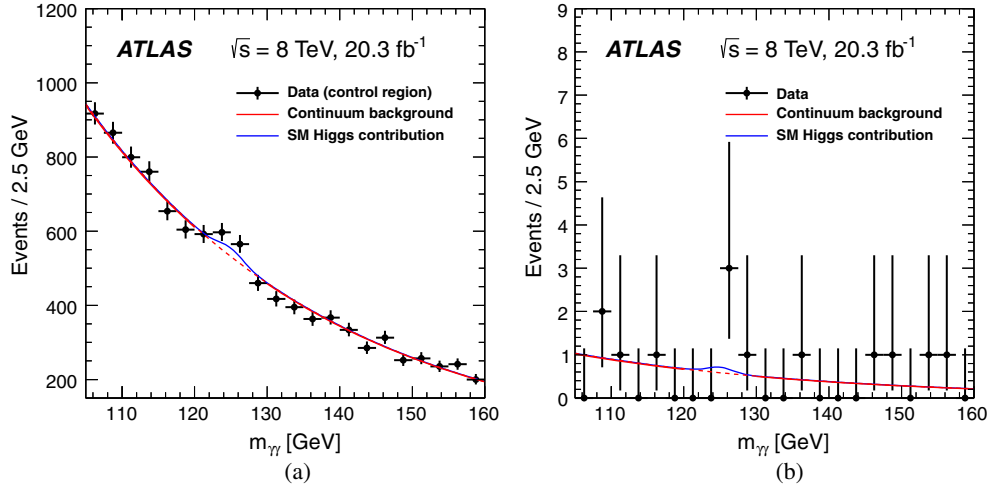
FIG. 4 (color online).   The distribution of the diphoton invariant mass for events passing (a) the relaxed requirements and (b) the final selection. The relaxed requirements include all final selections except those on the lepton and E_T^{miss}. The red curves represent the continuum background contributions and the blue curves include the contributions expected from single SM Higgs boson production estimated from simulation. The continuum background contributions in the signal $m_{\gamma\gamma}$ mass window are shown as dashed lines.

Here N_{SB}^{Data} is the number of events in the data sidebands, defined as the mass region $105 < m_{\gamma\gamma} < 160$ GeV excluding the signal region. The quantity f_{SB} is the fraction of background events in $105 < m_{\gamma\gamma} < 160$ GeV falling into the signal mass window, and can in principle be determined from a fit of the observed $m_{\gamma\gamma}$ distribution to an ansatz function. However, the small number of events after the final selection makes such a fit unsuitable. Instead, f_{SB} is determined in a data control sample, selected as the signal sample without the lepton and E_T^{miss} requirements. Figure 4(a) shows the $m_{\gamma\gamma}$ distribution of events in the control sample. For the fit, an exponential function is used to model the sidebands and a wider region of $m_h \pm 5$ GeV is excluded to minimize potential signal contamination in the sidebands. The fit yields a value of $f_{SB} = 0.1348 \pm 0.0001$. Varying the fit range of the sidebands leads to negligible changes. Different fit functions, such as a second-order polynomial or an exponentiated second-order polynomial, lead to a difference of 1.4% in f_{SB}. To study the sample dependence of f_{SB}, the fit is repeated for the control sample without the jet and E_T^{miss} requirements and a difference of only 2% is observed. Simulation studies show that the continuum background is dominated by $W(\ell\nu)\gamma\gamma +$ jets production. The $\gamma\gamma\ell\nu +$ jets events generated using MadGraph reproduce well the observed $m_{\gamma\gamma}$ distribution. The potential difference between $\gamma\gamma +$ jets and $\gamma\gamma\ell\nu +$ jets samples is studied using simulation. A difference below 1% is observed. Taking all these differences as systematic uncertainties, the fraction of background events in the signal mass window is $f_{SB} = 0.135 \pm 0.004$. With 9 (N_{SB}^{Data}) events observed in the data sidebands, it leads to $N_{SR}^{est} = 1.40 \pm 0.47$ events from the continuum background. Figure 4(a) also shows the contribution expected from single SM Higgs boson production. The data prefer

a larger cross section than the SM prediction for single Higgs boson production, consistent with the measurement reported in Ref. [66].

The uncertainties on the signal acceptances are estimated following the same procedure as the $hh \to bb\tau\tau$ analysis. The total experimental uncertainty is found to vary between 4% and 7% for different signal samples under consideration, dominated by the contribution from the jet energy scale. The theoretical uncertainties from PDFs, the renormalization and factorization scales, and the strong coupling constant are 3%, 1%, and 3%, respectively, the same as for the $hh \to bb\tau\tau$ analysis.

The $m_{\gamma\gamma}$ distribution of the selected events in the data is shown in Fig. 4(b). In total, 13 events are found with $105 < m_{\gamma\gamma} < 160$ GeV. Among them, 4 events are in the signal mass window of $m_h \pm 2\sigma$ compared with 1.65 ± 0.47 events expected from single SM Higgs boson production and continuum background processes. The p-value of the background-only hypothesis is 3.8%, corresponding to 1.8 standard deviations.

Assuming a cross section of 1 pb ($\sigma(gg \to hh)$ or $\sigma(gg \to H) \times BR(H \to hh)$) for Higgs boson pair production, the expected number of signal events is 0.64 ± 0.05 for the nonresonant production. For the resonant production, the corresponding numbers of events are 0.47 ± 0.05 and 0.72 ± 0.06 for a resonance mass of 300 GeV and 500 GeV, respectively. The implications of the search for Higgs boson pair production are discussed in Sec. IX.

VIII. COMBINATION PROCEDURE

The statistical analysis of the searches is based on the framework described in Refs. [67–70]. Profile-likelihood-ratio test statistics are used to measure the compatibility of the background-only hypothesis with the observed data

TABLE III.   An overview of the number of categories and final discriminant distributions used for both the nonresonant and resonant searches. Shown in the last column are the mass ranges of the resonant searches.

hh Final state	Nonresonant search Categories	Discriminant	Resonant search Categories	Discriminant	m_H [GeV]
$\gamma\gamma b\bar{b}$	1	$m_{\gamma\gamma}$	1	event yields	260–500
$\gamma\gamma WW^*$	1	event yields	1	event yields	260–500
$b\bar{b}\tau\tau$	4	$m_{\tau\tau}$	4	$m_{bb\tau\tau}$	260–1000
$b\bar{b}b\bar{b}$	1	event yields	1	m_{bbbb}	500–1500

and to test the hypothesis of Higgs boson pair production with its cross section as the parameter of interest. Additional nuisance parameters are included to take into account systematic uncertainties and their correlations. The likelihood is the product of terms of the Poisson probability constructed from the final discriminant and of nuisance parameter constraints with either Gaussian, log-normal, or Poisson distributions. Upper limits on the Higgs boson pair production cross section are derived using the CL_s method [71]. For the combinations, systematic uncertainties that affect two or more analyses (such as those of luminosity, jet energy scale and resolutions, b-tagging, etc.) are modeled with common nuisance parameters.

For the $hh \to bb\tau\tau$ analysis, Poisson probability terms are calculated for the four categories separately from the mass distributions of the ditau system for the nonresonant search [Fig. 3(a)] and of the $bb\tau\tau$ system for the resonant search [Fig. 3(b)]. The $m_{bb\tau\tau}$ distributions of the resonant search are rebinned to ensure a sufficient number of events for the background prediction in each bin, in particular a single bin is used for $m_{bb\tau\tau} \gtrsim 400$ GeV for each category. For the $hh \to \gamma\gamma WW^*$ analysis, event yields are used to calculate Poisson probabilities without exploiting shape information. The $hh \to \gamma\gamma bb$ and $hh \to bbbb$ analyses are published separately in Refs. [21,22]. However, the results are quoted at slightly different values of the Higgs boson mass m_h and, therefore, have been updated using a common mass value of $m_h = 125.4$ GeV [24] for the combinations. The decay branching ratios of the Higgs boson h and their uncertainties used in the combinations are taken from Ref. [27]. Table III is a summary of the number of categories and final discriminants used for each analysis.

The four individual analyses are sensitive to different kinematic regions of the hh production and decays. The combination is performed assuming that the relative contributions of these regions to the total cross section are modeled by the MadGraph5 [39] program used to simulate the hh production.

IX. RESULTS

In this section, the limits on the nonresonant and resonant searches are derived. The results of the $hh \to bb\tau\tau$ and $hh \to \gamma\gamma WW^*$ analyses are first determined and then combined with previously published results of the $hh \to \gamma\gamma bb$ and $hh \to bbbb$ analyses. The impact of the leading systematic uncertainties is also discussed.

The observed and expected upper limits at 95% C.L. on the cross section of nonresonant production of a Higgs boson pair are shown in Table IV. These limits are to be compared with the SM prediction of 9.9 ± 1.3 fb [17] for $gg \to hh$ production with $m_h = 125.4$ GeV. Only the gluon fusion production process is considered. The observed (expected) cross-section limits are 1.6 (1.3) pb and 11.4 (6.7) pb from the $hh \to bb\tau\tau$ and $hh \to \gamma\gamma WW^*$ analyses, respectively. Also shown in the table are the cross-section limits relative to the SM expectation. The results are combined with those of the $hh \to \gamma\gamma bb$ and $hh \to bbbb$ analyses. The p-value of compatibility of the combination with the SM hypothesis is 4.4%, equivalent to 1.7 standard deviations. The low p-value is a result of the excess of events observed in the $hh \to \gamma\gamma bb$ analysis. The combined observed (expected) upper limit on $\sigma(gg \to hh)$ is 0.69 (0.47) pb, corresponding to 70 (48) times the cross

TABLE IV.   The expected and observed 95% C.L. upper limits on the cross sections of nonresonant $gg \to hh$ production at $\sqrt{s} = 8$ TeV from individual analyses and their combinations. SM values are assumed for the h decay branching ratios. The cross-section limits normalized to the SM value are also included.

Analysis	$\gamma\gamma bb$	$\gamma\gamma WW^*$	$bb\tau\tau$	$bbbb$	Combined
Upper limit on the cross section [pb]					
Expected	1.0	6.7	1.3	0.62	0.47
Observed	2.2	11	1.6	0.62	0.69
Upper limit on the cross section relative to the SM prediction					
Expected	100	680	130	63	48
Observed	220	1150	160	63	70

TABLE V.   The impact of the leading systematic uncertainties on the signal-strength parameter μ of a hypothesized signal for both the nonresonant and resonant ($m_H = 300$, 600 GeV) searches. For the signal hypothesis, a Higgs boson pair production cross section [$\sigma(gg \rightarrow hh)$ or $\sigma(gg \rightarrow H) \times \mathrm{BR}(H \rightarrow hh)$] of 1 pb is assumed.

Nonresonant search		Resonant search			
		$m_H = 300$ GeV		$m_H = 600$ GeV	
Source	$\Delta\mu/\mu$ [%]	Source	$\Delta\mu/\mu$ [%]	Source	$\Delta\mu/\mu$ [%]
Background model	11	Background model	15	b-tagging	10
b-tagging	7.9	Jet and E_T^{miss}	9.9	h BR	6.3
h BR	5.8	Lepton and τ_{had}	6.9	Jet and E_T^{miss}	5.5
Jet and E_T^{miss}	5.5	h BR	5.9	Luminosity	2.7
Luminosity	3.0	Luminosity	4.0	Background model	2.4
Total	16	Total	21	Total	14

section predicted by the SM. The $hh \rightarrow bbbb$ analysis has the best expected sensitivity followed by the $hh \rightarrow \gamma\gamma bb$ analysis. The observed combined limit is slightly weaker than that of the $hh \rightarrow bbbb$ analysis, largely due to the aforementioned excess.

The impact of systematic uncertainties on the cross-section limits is studied using the signal-strength parameter μ, defined as the ratio of the extracted to the assumed signal cross section [times branching ratio $\mathrm{BR}(H \rightarrow hh)$ for the resonant search]. The resulting shifts in μ depend on the actual signal-strength value. For illustration, they are evaluated using a cross section of 1 pb for $gg \rightarrow (H \rightarrow)hh$, comparable to the limits set. The effects of the most important uncertainty sources are shown in Table V. The leading contributions are from the background modeling, b-tagging, the h decay branching ratios, jet and E_T^{miss} measurements. The large impact of the b-tagging systematic uncertainty reflects the relatively large weight of the $hh \rightarrow bbbb$ analysis in the combination. For the $hh \rightarrow bb\tau\tau$ analysis alone, the three leading systematic sources are the background estimates, jet and E_T^{miss} measurements, and lepton and τ_{had} identifications. For the $hh \rightarrow \gamma\gamma WW^*$

analysis, they are the background estimates, jet and E_T^{miss} measurements and theoretical uncertainties of the decay branching ratios of the Higgs boson h.

For the resonant production, limits are set on the cross section of $gg \rightarrow H$ production of the heavy Higgs boson times its branching ratio $\mathrm{BR}(H \rightarrow hh)$ as a function of the heavy Higgs boson mass m_H. The observed (expected) limits of the $hh \rightarrow bb\tau\tau$ and $hh \rightarrow \gamma\gamma WW^*$ analyses are illustrated in Fig. 5 and listed in Table VI (along with results from the $hh \rightarrow \gamma\gamma bb$ and $hh \rightarrow bbbb$ analyses). The m_H search ranges are 260–1000 GeV for $hh \rightarrow bb\tau\tau$ and 260–500 GeV for $hh \rightarrow \gamma\gamma WW^*$. For the $hh \rightarrow bb\tau\tau$ analysis, the observed limit around $m_H \sim 300$ GeV is considerably lower than the expectation, reflecting the deficit in the observed $m_{bb\tau\tau}$ distribution. At high mass, the limits are correlated since a single bin is used for $m_{bb\tau\tau} \gtrsim 400$ GeV. The decrease in the limit as m_H increases is a direct consequence of increasing selection efficiency for the signal. This is also true for the $hh \rightarrow \gamma\gamma WW^*$ analysis as the event selection is independent of m_H.

The $hh \rightarrow \gamma\gamma bb$ and $hh \rightarrow bbbb$ analyses are published separately and the mass range covered by the two analyses
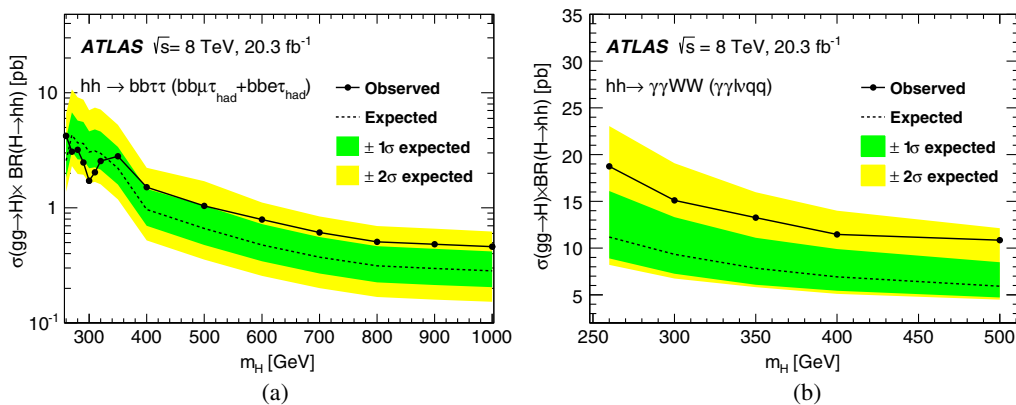

FIG. 5 (color online).   The observed and expected upper limit at 95% C.L. on $\sigma(gg \rightarrow H) \times \mathrm{BR}(H \rightarrow hh)$ at $\sqrt{s} = 8$ TeV as a function of m_H from the resonant (a) $hh \rightarrow bb\tau\tau$ and (b) $hh \rightarrow \gamma\gamma WW^*$ analyses. The search ranges of the resonance mass are 260–1000 GeV for $hh \rightarrow bb\tau\tau$ and 260–500 GeV for $hh \rightarrow \gamma\gamma WW^*$. The green and yellow bands represent $\pm 1\sigma$ and $\pm 2\sigma$ ranges on the expected limits, respectively.

TABLE VI. The expected and observed 95% C.L. upper limits on $\sigma(gg \to H) \times \mathrm{BR}(H \to hh)$ in pb at $\sqrt{s} = 8$ TeV from individual analyses and their combinations. The SM branching ratios are assumed for the light Higgs boson decay.

m_H [GeV]	Expected limit [pb]					Observed limit [pb]				
	$\gamma\gamma bb$	$\gamma\gamma WW^*$	$bb\tau\tau$	$bbbb$	Combined	$\gamma\gamma bb$	$\gamma\gamma WW^*$	$bb\tau\tau$	$bbbb$	Combined
260	1.70	11.2	2.6	⋯	1.1	2.29	18.7	4.2	⋯	2.1
300	1.53	9.3	3.1	⋯	1.2	3.54	15.1	1.7	⋯	2.0
350	1.23	7.8	2.2	⋯	0.89	1.44	13.3	2.8	⋯	1.5
400	1.00	6.9	0.97	⋯	0.56	1.00	11.5	1.5	⋯	0.83
500	0.72	5.9	0.66	⋯	0.38	0.71	10.9	1.0	⋯	0.61
500	⋯	⋯	0.66	0.17	0.16	⋯	⋯	1.0	0.16	0.18
600	⋯	⋯	0.48	0.070	0.067	⋯	⋯	0.79	0.072	0.079
700	⋯	⋯	0.31	0.041	0.040	⋯	⋯	0.61	0.038	0.040
800	⋯	⋯	0.31	0.028	0.028	⋯	⋯	0.51	0.046	0.049
900	⋯	⋯	0.30	0.022	0.022	⋯	⋯	0.48	0.015	0.015
1000	⋯	⋯	0.28	0.018	0.018	⋯	⋯	0.46	0.011	0.011

are 260–500 GeV and 500–1500 GeV, respectively. The results of these four analyses, summarized in Table VI, are combined for the mass range 260–1000 GeV assuming the SM values of the h decay branching ratios. To reflect the better mass resolutions of the $hh \to bbbb$ and $hh \to \gamma\gamma bb$ analyses, the combination is performed with smaller mass steps than those of the $hh \to bb\tau\tau$ and $hh \to \gamma\gamma WW^*$ analyses. The most significant excess in the combined results is at a resonance mass of 300 GeV with a local significance of 2.5σ, largely due to the 3.0σ excess observed in the $hh \to \gamma\gamma bb$ analysis [21]. The upper limit on $\sigma(gg \to H) \times \mathrm{BR}(H \to hh)$ varies from 2.1 pb at

FIG. 6 (color online). The observed and expected 95% C.L. upper limits on $\sigma(gg \to H) \times \mathrm{BR}(H \to hh)$ at $\sqrt{s} = 8$ TeV as functions of the heavy Higgs boson mass m_H, combining resonant searches in $hh \to \gamma\gamma bb$, $bbbb$, $bb\tau\tau$, and $\gamma\gamma WW^*$ final states. The expected limits from individual analyses are also shown. The combination assumes SM values for the decay branching ratios of the lighter Higgs boson h. The green and yellow bands represent $\pm 1\sigma$ and $\pm 2\sigma$ uncertainty ranges of the expected combined limits. The improvement above $m_H = 500$ GeV is due to the sensitivity of the $hh \to bbbb$ analysis. The more finely spaced mass points of the combination reflect the better mass resolutions of the $hh \to \gamma\gamma bb$ and $hh \to bbbb$ analyses than those of $hh \to bb\tau\tau$ and $hh \to \gamma\gamma WW^*$ analyses.

260 GeV to 0.011 pb at 1000 GeV. These limits are shown in Fig. 6 as a function of m_H. For the low-mass region of 260–500 GeV, both the $hh \to \gamma\gamma bb$ and $hh \to bb\tau\tau$ analyses contribute significantly to the combined sensitivities. Above 500 GeV, the sensitivity is dominated by the $hh \to bbbb$ analysis. Table V shows the impact of the leading systematic uncertainties for a heavy Higgs boson mass of 300 and 600 GeV. As in the nonresonant search, the systematic uncertainties with the largest impact on the sensitivity are from the uncertainties on the background modeling, b-tagging, jet and $E_{\mathrm{T}}^{\mathrm{miss}}$ measurements, and the h decay branching ratios. These limits are directly applicable to models such as those of Refs. [72–77] in which the Higgs boson h has the same branching ratios as the SM Higgs boson.
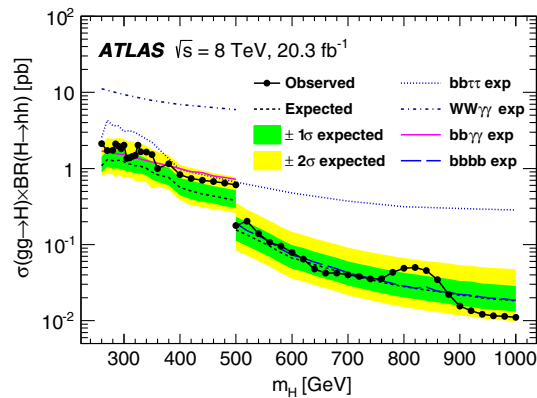
X. INTERPRETATION

The upper cross-section limits of the resonant search are interpreted in two MSSM scenarios, one referred to as the hMSSM [28,29] and the other as the low-tb-high [30]. In the interpretation, the CP-even light and heavy Higgs bosons of the MSSM are assumed to be the Higgs bosons h and H of the search, respectively. The natural width of the heavy Higgs boson H where limits are set in these scenarios is sufficiently smaller than the experimental resolution, which is at best 1.5%, that its effect can be neglected.

In the hMSSM scenario, the mass of the light CP-even Higgs boson is fixed to 125 GeV in the whole parameter space. This is achieved by implicitly allowing the supersymmetry-breaking scale m_S to be very large, which is especially true in the low $\tan\beta$ region where $m_S \gg 1$ TeV, and making assumptions about the CP-even Higgs boson mass matrix and its radiative corrections, as well as the Higgs boson coupling dependence on the MSSM parameters. Here $\tan\beta$ is the ratio of the vacuum expectation values of the two doublet Higgs fields. The "low-tb-high" MSSM scenario follows a similar approach, differing in that explicit choices are made for the supersymmetry-breaking
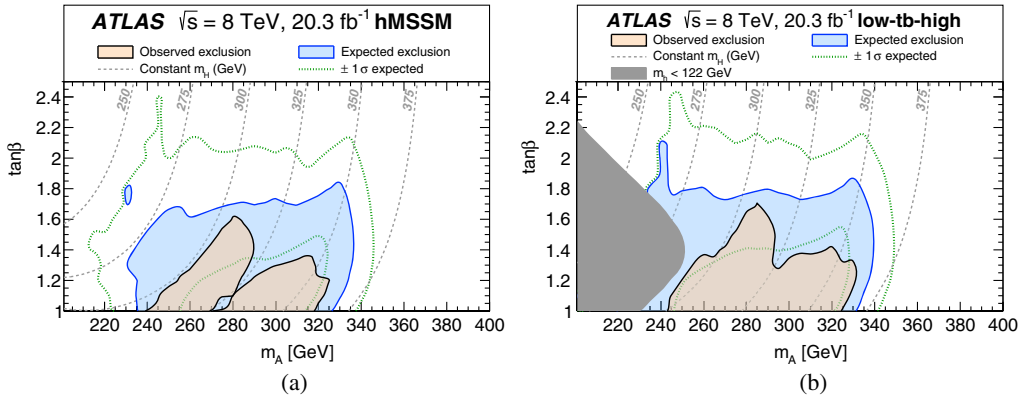
FIG. 7 (color online).   The observed and expected 95% C.L. exclusion regions in the $(\tan\beta, m_A)$ plane of MSSM scenarios from the resonant search: (a) the hMSSM scenario and (b) the low-tb-high scenario. The green dotted lines delimit the $\pm 1\sigma$ uncertainty ranges of the expected exclusion regions. The gray dashed lines show the constant values of the heavy CP-even Higgs boson mass. The improved sensitivity in the expected exclusion on the contour line of $m_H \sim 260$ GeV reflects the improved expected limit on the cross section while the hole or the wedge around the $m_H \sim 325$ GeV contour line in the observed exclusion is the result of a small excess at this mass; see Fig. 6. The gray shaded region in (b) shows the region where the mass of the light CP-even Higgs boson is inconsistent with the measured value of 125.4 GeV. There is no such region in (a) by construction.

parameters [30]. The mass of the light Higgs boson is not fixed in this scenario, but is approximately 125 GeV in most of the parameter space. The m_h value grows gradually from 122 GeV at $m_A \sim 220$ GeV to 125 GeV as m_A approaching infinity. Higgs boson production cross sections through the gluon-fusion process are calculated with SʊSHi 1.4.1 [78–80] for both scenarios. Higgs boson decay branching ratios are calculated with HDECAY 6.42 [81] following the prescription of Ref. [29] for the hMSSM scenario and with FᴇʏɴHɪɢɢs 2.10.0 [82–84] for the low-tb-high scenario.

The upper limits on $\sigma(gg \to H) \times \mathrm{BR}(H \to hh)$ can be interpreted as exclusion regions in the $(\tan\beta, m_A)$ plane. In both scenarios, the Higgs boson pair production rate $\sigma(gg \to H) \times \mathrm{BR}(H \to hh)$ depends on $\tan\beta$ and the mass of the CP-odd Higgs boson (m_A), and so does the mass of the heavy CP-even Higgs boson H. The values of m_A and m_H are generally different: m_H can be as much as 70 GeV above m_A in the parameter space relevant for this publication with the difference in masses decreasing for increasing values of $\tan\beta$ or m_A. Constant m_H lines for a few selected values are shown in Fig. 7. The decay branching ratios of the light Higgs boson in these scenarios depend on $\tan\beta$ and m_A and are different from the corresponding SM values used to derive the upper limits shown in Table VI. The upper limits, as functions of m_H, are recomputed; the hh decay fractions for each final state are fixed to their smallest value found in $1 < \tan\beta < 2$, the range of the expected sensitivity. This approach yields conservative limits, but simplifies the computation as the limit calculation does not have to be repeated at each $\tan\beta$ value. The results are used to set exclusions in the $(\tan\beta, m_A)$ plane as shown in Fig. 7. The analysis is sensitive to the region of low $\tan\beta$ and m_A values in the range $\sim 200 - 350$ GeV. For $m_A \lesssim 200$ GeV, m_H is typically below the $2m_h$ threshold of the $H \to hh$

decay, whereas above 350 GeV, the $H \to hh$ decay is suppressed because of the dominance of the $H \to t\bar{t}$ decay. The observed exclusion region in the $(\tan\beta, m_A)$ plane is smaller than the expectation, reflecting the small excess observed in the data.

XI. SUMMARY

This paper summarizes the search for both nonresonant and resonant Higgs boson pair production in proton-proton collisions from approximately 20 fb^{-1} of data at a center-of-mass energy of 8 TeV recorded by the ATLAS detector at the LHC. The search is performed in $hh \to bb\tau\tau$ and $\gamma\gamma WW^*$ final states. No significant excess is observed in the data beyond the background expectation. Upper limits on the hh production cross section are derived. Combining with the $hh \to \gamma\gamma bb$, $bbbb$ searches, a 95% C.L. upper limit of 0.69 pb on the cross section of the nonresonant hh production is observed compared with the expected limit of 0.47 pb. This observed upper limit is approximately 70 times the SM $gg \to hh$ production cross section. For the production of a narrow heavy resonance decaying to a pair of light Higgs bosons, the observed (expected) upper limit on $\sigma(gg \to H) \times \mathrm{BR}(H \to hh)$ varies from 2.1 (1.1) pb at 260 GeV to 0.011 (0.018) pb at 1000 GeV. These limits are obtained assuming SM values for the h decay branching ratios. Exclusion regions in the parameter space of simplified MSSM scenarios are also derived.

[1] ATLAS Collaboration, Observation of a new particle in the search for the standard model Higgs boson with the ATLAS detector at the LHC, Phys. Lett. B **716**, 1 (2012).

[2] CMS Collaboration, Observation of a new boson at a mass of 125 GeV with the CMS experiment at the LHC, Phys. Lett. B **716**, 30 (2012).

[3] ATLAS Collaboration, Measurements of Higgs boson production and couplings in diboson final states with the ATLAS detector at the LHC, Phys. Lett. B **726**, 88 (2013).

[4] CMS Collaboration, Precise determination of the mass of the Higgs boson and tests of compatibility of its couplings with the standard model predictions using proton collisions at 7 and 8 TeV, Eur. Phys. J. C **75**, 212 (2015).

[5] ATLAS Collaboration, Search for the $b\bar{b}$ decay of the standard model Higgs boson in associated $(W/Z)H$ production with the ATLAS detector, J. High Energy Phys. 01 (2015) 069.

[6] ATLAS Collaboration, Evidence for the Higgs-boson Yukawa coupling to tau leptons with the ATLAS detector, J. High Energy Phys. 04 (2015) 117.

[7] ATLAS Collaboration, Evidence for the spin-0 nature of the Higgs boson using ATLAS data, Phys. Lett. B **726**, 120 (2013).

[8] CMS Collaboration, Constraints on the spin-parity and anomalous HVV couplings of the Higgs boson in proton collisions at 7 and 8 TeV, Phys. Rev. D **92**, 012004 (2015).

[9] U. Baur, T. Plehn, and D. L. Rainwater, Determining the Higgs boson self-coupling at hadron colliders, Phys. Rev. D **67**, 033003 (2003).

[10] U. Baur, T. Plehn, and D. L. Rainwater, Probing the Higgs self-coupling at hadron colliders using rare decays, Phys. Rev. D **69**, 053004 (2004).

[11] M. J. Dolan, C. Englert, and M. Spannowsky, Higgs self-coupling measurements at the LHC, J. High Energy Phys. 10 (2012) 112.

[12] J. Baglio, A. Djouadi, R. Gröber, M. M. Mühlleitner, J. Quevillon, and M. Spira, The measurement of the Higgs self-coupling at the LHC: Theoretical status, J. High Energy Phys. 04 (2013) 151.

[13] L.-C. Lu et al., Searching for heavier Higgs boson via di-Higgs production at LHC run-2, arXiv:1507.02644.

[14] S. Dawson et al., Higgs Working Group report, arXiv:1310.8361.

[15] S. Dawson, S. Dittmaier, and M. Spira, Neutral Higgs-boson pair production at hadron colliders: QCD corrections, Phys. Rev. D **58**, 115012 (1998).

[16] J. Grigo, J. Hoff, K. Melnikov, and M. Steinhauser, On the Higgs boson pair production at the LHC, Nucl. Phys. **B875**, 1 (2013).

[17] D. de Florian and J. Mazzitelli, Higgs Boson Pair Production at Next-to-Next-to-Leading Order in QCD, Phys. Rev. Lett. **111**, 201801 (2013).

[18] H. E. Haber and G. L. Kane, The search for supersymmetry: Probing physics beyond the standard model, Phys. Rep. **117**, 75 (1985).

[19] R. Grober and M. Muhlleitner, Composite Higgs boson pair production at the LHC, J. High Energy Phys. 06 (2011) 020.

[20] R. Contino, M. Ghezzi, M. Moretti, G. Panico, F. Piccinini, and A. Wulzer, Anomalous couplings in double Higgs production, J. High Energy Phys. 08 (2012) 154.

[21] ATLAS Collaboration, Search for Higgs Boson Pair Production in the $\gamma\gamma b\bar{b}$ Final State Using pp Collision Data at $\sqrt{s} = 8$ TeV from the ATLAS Detector, Phys. Rev. Lett. **114**, 081802 (2015).

[22] ATLAS Collaboration, Search for Higgs boson pair production in the $b\bar{b}b\bar{b}$ final state from pp collisions at $\sqrt{s} = 8$ TeV with the ATLAS detector, Eur. Phys. J. C 75, 412 (2015).

[23] CMS Collaboration, Search for resonant pair production of Higgs bosons decaying to two bottom quark-antiquark pairs in proton-proton collisions at 8 TeV, Phys. Lett. B 749, 560 (2015).

[24] ATLAS Collaboration, Measurement of the Higgs boson mass from the $H \to \gamma\gamma$ and $H \to ZZ^* \to 4\ell$ channels in pp collisions at center-of-mass energies of 7 and 8 TeV with the ATLAS detector, Phys. Rev. D 90, 052004 (2014).

[25] S. Dittmaier et al., Handbook of LHC Higgs cross sections: 1. Inclusive observables, arXiv:1101.0593.

[26] S. Dittmaier et al., Handbook of LHC Higgs cross sections: 2. Differential distributions, arXiv:1201.3084.

[27] S. Heinemeyer et al., Handbook of LHC Higgs cross sections: 3. Higgs properties, arXiv:1307.1347.

[28] A. Djouadi, L. Maiani, G. Moreau, A. Polosa, J. Quevillon, and V. Riquer, The post-Higgs MSSM scenario: Habemus MSSM?, Eur. Phys. J. C 73, 2650 (2013).

[29] A. Djouadi, L. Maiani, A. Polosa, J. Quevillon, and V. Riquer, Fully covering the MSSM Higgs sector at the LHC, J. High Energy Phys. 06 (2015) 168.

[30] E. Bagnaschi et al., CERN Report No. LHCHXSWG-2015-002, 2015, http://cds.cern.ch/record/2039911.

[31] ATLAS Collaboration, The ATLAS experiment at the CERN Large Hadron Collider, JINST 3, S08003 (2008).

[32] T. Sjostrand, S. Mrenna, and P. Z. Skands, A brief introduction to PYTHIA 8.1, Comput. Phys. Commun. 178, 852 (2008).

[33] H.-L. Lai, M. Guzzi, J. Huston, Z. Li, P. M. Nadolsky, J. Pumplin, and C.-P. Yuan, New parton distributions for collider physics, Phys. Rev. D 82, 074024 (2010).

[34] J. Pumplin, D. R. Stump, J. Huston, H.-L. Lai, P. Nadolsky, and W.-K. Tung, New Generation of Parton Distributions with Uncertainties from Global QCD Analysis, J. High Energy Phys. 07 (2002) 012.

[35] A. D. Martin, W. J. Stirling, R. S. Thorne, and G. Watt, Parton distributions for the LHC, Eur. Phys. J. C 63, 189 (2009).

[36] R. D. Ball et al., Parton distribution benchmarking with LHC data, J. High Energy Phys. 04 (2013) 125.

[37] ATLAS Collaboration, The ATLAS simulation infrastructure, Eur. Phys. J. C 70, 823 (2010).

[38] S. Agostinelli et al., GEANT4: A simulation toolkit, Nucl. Instrum. Methods Phys. Res., Sect. A 506, 250 (2003).

[39] J. Alwall, M. Herquet, F. Maltoni, O. Mattelaer, and T. Stelzer, MadGraph 5: Going beyond, J. High Energy Phys. 06 (2011) 128.

[40] T. Plehn, M. Spira, and P. Zerwas, Pair production of neutral Higgs particles in gluon-gluon collisions, Nucl. Phys. B479, 46 (1996).

[41] R. Frederix, S. Frixione, V. Hirschi, F. Maltoni, O. Mattelaer, P. Torrielli, E. Vryonidou, and M. Zaro, Higgs pair production at the LHC with NLO and parton-shower effects, Phys. Lett. B 732, 142 (2014).

[42] B. Hespel and E. Vryonidou, Higgs Pair Production, http://cp3.irmp.ucl.ac.be/projects/madgraph/wiki/HiggsPairProduction.

[43] P. Nason, A new method for combining NLO QCD with shower Monte Carlo algorithms, J. High Energy Phys. 11 (2004) 040.

[44] S. Frixione, P. Nason, and C. Oleari, Matching NLO QCD computations with parton shower simulations: The POWHEG method, J. High Energy Phys. 11 (2007) 070.

[45] S. Alioli, P. Nason, C. Oleari, and E. Re, A general framework for implementing NLO calculations in shower Monte Carlo programs: The POWHEG BOX, J. High Energy Phys. 06 (2010) 043.

[46] M. Grazzini and H. Sargsyan, Heavy-quark mass effects in Higgs boson production at the LHC, J. High Energy Phys. 09 (2013) 129.

[47] D. de Florian, G. Ferrera, M. Grazzini, and D. Tommasini, Higgs boson production at the LHC: Transverse momentum resummation effects in the $H \to 2\gamma$, $H \to WW \to \ell\nu\ell'\nu'$ and $H \to ZZ \to 4\ell$ decay modes, J. High Energy Phys. 06 (2012) 132.

[48] M. L. Mangano, F. Piccinini, A. D Polosa, M. Moretti, and R. Pittau, ALPGEN, a generator for hard multiparton processes in hadronic collisions, J. High Energy Phys. 07 (2003) 001.

[49] B. P. Kersevan and E. Richter-Was, The Monte Carlo event generator AcerMC versions 2.0 to 3.8 with interfaces to PYTHIA 6.4, HERWIG 6.5 and ARIADNE 4.1, Comput. Phys. Commun. 184, 919 (2013).

[50] M. Czakon, P. Fiedler, and A. Mitov, Total Top-Quark Pair-Production Cross Section at Hadron Colliders through $O(\alpha_S^4)$, Phys. Rev. Lett. 110, 252004 (2013).

[51] N. Kidonakis, Next-to-next-to-leading-order collinear and soft gluon corrections for t-channel single top quark production, Phys. Rev. D 83, 091503 (2011).

[52] N. Kidonakis, Next-to-next-to-leading logarithm resummation for s-channel single top quark production, Phys. Rev. D 81, 054028 (2010).

[53] N. Kidonakis, Two-loop soft anomalous dimensions for single top quark associated production with a W^- or H^-, Phys. Rev. D 82, 054018 (2010).

[54] J. M. Campbell and R. Ellis, MCFM for the Tevatron and the LHC, Nucl. Phys. B, Proc. Suppl. 205–206, 10 (2010).

[55] J. M. Campbell, R. K. Ellis, and C. Williams, Vector boson pair production at the LHC, J. High Energy Phys. 07 (2011) 018.

[56] ATLAS Collaboration, Measurement of Higgs boson production in the diphoton decay channel in pp collisions at center-of-mass energies of 7 and 8 TeV with the ATLAS detector, Phys. Rev. D 90, 112015 (2014).

[57] ATLAS Collaboration, ATLAS Report No. ATLAS-CONF-2014-032, 2014, http://cds.cern.ch/record/1706245.

[58] ATLAS Collaboration, ATLAS Report No. ATLAS-CONF-2012-123, 2012, http://cds.cern.ch/record/1473426.

[59] M. Cacciari, G. P. Salam, and G. Soyez, The anti-k_t jet clustering algorithm, J. High Energy Phys. 04 (2008) 063.

[60] ATLAS Collaboration, ATLAS Report No. ATLAS-CONF-2014-046, 2014, http://cds.cern.ch/record/1741020.

[61] ATLAS Collaboration, Identification and energy calibration of hadronically decaying tau leptons with the ATLAS experiment in pp collisions at $\sqrt{s} = 8$ TeV, Eur. Phys. J. C 75, 303 (2015).

[62] ATLAS Collaboration, Performance of missing transverse momentum reconstruction in proton-proton collisions at 7 TeV with ATLAS, Eur. Phys. J. C 72, 1844 (2012).

[63] ATLAS Collaboration, Modelling $Z \to \tau\tau$ processes in ATLAS with τ-embedded $Z \to \mu\mu$ data, JINST 10, P09018 (2015).

[64] ATLAS Collaboration, Measurements of normalized differential cross sections for $t\bar{t}$ production in pp collisions at $\sqrt{s} = 7$ TeV using the ATLAS detector, Phys. Rev. D 90, 072004 (2014).

[65] A. Elagin, P. Murat, A. Pranko, and A. Safonov, A new mass reconstruction technique for resonances decaying to $\tau\tau$, Nucl. Instrum. Methods Phys. Res., Sect. A 654, 481 (2011).

[66] ATLAS Collaboration, Measurements of fiducial and differential cross sections for Higgs boson production in the diphoton decay channel at $\sqrt{s} = 8$ TeV with ATLAS, J. High Energy Phys. 09 (2014) 112.

[67] ATLAS Collaboration, Combined search for the Standard Model Higgs boson in pp collisions at $\sqrt{s} = 7$ TeV with the ATLAS detector, Phys. Rev. D 86, 032003 (2012).

[68] L. Moneta et al., The RooStats Project, Proc. Sci., ACAT2010 (2010) 057.

[69] W. Verkerke and D. P. Kirkby, The RooFit toolkit for data modeling, eConf C0303241 (2003), p. MOLT007; http://inspirehep.net/record/621398.

[70] G. Cowan, K. Cranmer, E. Gross, and O. Vitells, Asymptotic formulae for likelihood-based tests of new physics, Eur. Phys. J. C 71, 11554 (2011).

[71] A. L. Read, Presentation of search results: The CL_s technique, J. Phys. G 28, 2693 (2002).

[72] A. Hill and J. J. van der Bij, Strongly interacting singlet-double Higgs model, Phys. Rev. D 36, 3463 (1987).

[73] T. Binoth and J. J. van der Bij, Influence of strongly coupled, hidden scalars on Higgs signals, Z. Phys. C 75, 17 (1997).

[74] R. Schabinger and J. D. Wells, Minimal spontaneously broken hidden sector and its impact on Higgs boson physics at the CERN Large Hadron Collider, Phys. Rev. D 72, 093007 (2005).

[75] B. Patt and F. Wilczek, Higgs-field portal into hidden sectors, arXiv:hep-ph/0605188.

[76] G. M. Pruna and T. Robens, Higgs singlet extension parameter space in the light of the LHC discovery, Phys. Rev. D 88, 115012 (2013).

[77] T. Robens and T. Stefaniak, Status of the Higgs singlet extension of the standard model after LHC run 1, Eur. Phys. J. C 75, 104 (2015).

[78] R. V. Harlander, S. Liebler, and H. Mantler, SusHi: A program for the calculation of Higgs production in gluon fusion and bottom-quark annihilation in the Standard Model and the MSSM, Comput. Phys. Commun. 184, 1605 (2013).

[79] R. V. Harlander and W. B. Kilgore, Next-to-Next-to-Leading Order Higgs Production at Hadron Colliders, Phys. Rev. Lett. 88, 201801 (2002).

[80] U. Aglietti, R. Bonciani, G. Degrassi, and A. Vicini, Two-loop light fermion contribution to Higgs production and decays, Phys. Lett. B 595, 432 (2004).

[81] A. Djouadi, J. Kalinowski, and M. Spira, HDECAY: A program for Higgs boson decays in the Standard Model and its supersymmetric extension, Comput. Phys. Commun. 108, 56 (1998).

[82] S. Heinemeyer, W. Hollik, and G. Weiglein, FeynHiggs: A program for the calculation of the masses of the neutral CP-even Higgs bosons in the MSSM, Comput. Phys. Commun. 124, 76 (2000).

[83] G. Degrassi, S. Heinemeyer, W. Hollik, P. Slavich, and G. Weiglein, Towards high-precision predictions for the MSSM Higgs sector, Eur. Phys. J. C 28, 133 (2003).

[84] T. Hahn, S. Heinemeyer, W. Hollik, H. Rzehak, and G. Weiglein, High-Precision Predictions for the Light CP-Even Higgs Boson Mass of the Minimal Supersymmetric Standard Model, Phys. Rev. Lett. 112, 141801 (2014).

G. Aad,[85] B. Abbott,[113] J. Abdallah,[151] O. Abdinov,[11] R. Aben,[107] M. Abolins,[90] O. S. AbouZeid,[158] H. Abramowicz,[153] H. Abreu,[152] R. Abreu,[116] Y. Abulaiti,[146a,146b] B. S. Acharya,[164a,164b,b] L. Adamczyk,[38a] D. L. Adams,[25] J. Adelman,[108] S. Adomeit,[100] T. Adye,[131] A. A. Affolder,[74] T. Agatonovic-Jovin,[13] J. Agricola,[54] J. A. Aguilar-Saavedra,[126a,126f] S. P. Ahlen,[22] F. Ahmadov,[65,c] G. Aielli,[133a,133b] H. Akerstedt,[146a,146b] T. P. A. Åkesson,[81] A. V. Akimov,[96] G. L. Alberghi,[20a,20b] J. Albert,[169] S. Albrand,[55] M. J. Alconada Verzini,[71] M. Aleksa,[30] I. N. Aleksandrov,[65] C. Alexa,[26b] G. Alexander,[153] T. Alexopoulos,[10] M. Alhroob,[113] G. Alimonti,[91a] L. Alio,[85] J. Alison,[31] S. P. Alkire,[35] B. M. M. Allbrooke,[149] P. P. Allport,[18] A. Aloisio,[104a,104b] A. Alonso,[36] F. Alonso,[71] C. Alpigiani,[138] A. Altheimer,[35] B. Alvarez Gonzalez,[30] D. Álvarez Piqueras,[167] M. G. Alviggi,[104a,104b] B. T. Amadio,[15] K. Amako,[66] Y. Amaral Coutinho,[24a] C. Amelung,[23] D. Amidei,[89] S. P. Amor Dos Santos,[126a,126c] A. Amorim,[126a,126b] S. Amoroso,[48] N. Amram,[153] G. Amundsen,[23] C. Anastopoulos,[139] L. S. Ancu,[49] N. Andari,[108] T. Andeen,[35] C. F. Anders,[58b] G. Anders,[30] J. K. Anders,[74] K. J. Anderson,[31] A. Andreazza,[91a,91b] V. Andrei,[58a] S. Angelidakis,[9] I. Angelozzi,[107] P. Anger,[44] A. Angerami,[35] F. Anghinolfi,[30] A. V. Anisenkov,[109,d] N. Anjos,[12] A. Annovi,[124a,124b] M. Antonelli,[47] A. Antonov,[98] J. Antos,[144b] F. Anulli,[132a] M. Aoki,[66] L. Aperio Bella,[18] G. Arabidze,[90] Y. Arai,[66] J. P. Araque,[126a] A. T. H. Arce,[45] F. A. Arduh,[71] J-F. Arguin,[95] S. Argyropoulos,[63] M. Arik,[19a] A. J. Armbruster,[30] O. Arnaez,[30] H. Arnold,[48] M. Arratia,[28] O. Arslan,[21] A. Artamonov,[97] G. Artoni,[23] S. Asai,[155] N. Asbah,[42] A. Ashkenazi,[153] B. Åsman,[146a,146b] L. Asquith,[149] K. Assamagan,[25] R. Astalos,[144a] M. Atkinson,[165] N. B. Atlay,[141] K. Augsten,[128] M. Aurousseau,[145b] G. Avolio,[30] B. Axen,[15] M. K. Ayoub,[117]

G. Azuelos,[95,e] M. A. Baak,[30] A. E. Baas,[58a] M. J. Baca,[18] C. Bacci,[134a,134b] H. Bachacou,[136] K. Bachas,[154] M. Backes,[30] M. Backhaus,[30] P. Bagiacchi,[132a,132b] P. Bagnaia,[132a,132b] Y. Bai,[33a] T. Bain,[35] J. T. Baines,[131] O. K. Baker,[176] E. M. Baldin,[109,d] P. Balek,[129] T. Balestri,[148] F. Balli,[84] W. K. Balunas,[122] E. Banas,[39] Sw. Banerjee,[173] A. A. E. Bannoura,[175] L. Barak,[30] E. L. Barberio,[88] D. Barberis,[50a,50b] M. Barbero,[85] T. Barillari,[101] M. Barisonzi,[164a,164b] T. Barklow,[143] N. Barlow,[28] S. L. Barnes,[84] B. M. Barnett,[131] R. M. Barnett,[15] Z. Barnovska,[5] A. Baroncelli,[134a] G. Barone,[23] A. J. Barr,[120] F. Barreiro,[82] J. Barreiro Guimarães da Costa,[57] R. Bartoldus,[143] A. E. Barton,[72] P. Bartos,[144a] A. Basalaev,[123] A. Bassalat,[117] A. Basye,[165] R. L. Bates,[53] S. J. Batista,[158] J. R. Batley,[28] M. Battaglia,[137] M. Bauce,[132a,132b] F. Bauer,[136] H. S. Bawa,[143,f] J. B. Beacham,[111] M. D. Beattie,[72] T. Beau,[80] P. H. Beauchemin,[161] R. Beccherle,[124a,124b] P. Bechtle,[21] H. P. Beck,[17,g] K. Becker,[120] M. Becker,[83] M. Beckingham,[170] C. Becot,[117] A. J. Beddall,[19b] A. Beddall,[19b] V. A. Bednyakov,[65] C. P. Bee,[148] L. J. Beemster,[107] T. A. Beermann,[30] M. Begel,[25] J. K. Behr,[120] C. Belanger-Champagne,[87] W. H. Bell,[49] G. Bella,[153] L. Bellagamba,[20a] A. Bellerive,[29] M. Bellomo,[86] K. Belotskiy,[98] O. Beltramello,[30] O. Benary,[153] D. Benchekroun,[135a] M. Bender,[100] K. Bendtz,[146a,146b] N. Benekos,[10] Y. Benhammou,[153] E. Benhar Noccioli,[49] J. A. Benitez Garcia,[159b] D. P. Benjamin,[45] J. R. Bensinger,[23] S. Bentvelsen,[107] L. Beresford,[120] M. Beretta,[47] D. Berge,[107] E. Bergeaas Kuutmann,[166] N. Berger,[5] F. Berghaus,[169] J. Beringer,[15] C. Bernard,[22] N. R. Bernard,[86] C. Bernius,[110] F. U. Bernlochner,[21] T. Berry,[77] P. Berta,[129] C. Bertella,[83] G. Bertoli,[146a,146b] F. Bertolucci,[124a,124b] C. Bertsche,[113] D. Bertsche,[113] M. I. Besana,[91a] G. J. Besjes,[36] O. Bessidskaia Bylund,[146a,146b] M. Bessner,[42] N. Besson,[136] C. Betancourt,[48] S. Bethke,[101] A. J. Bevan,[76] W. Bhimji,[15] R. M. Bianchi,[125] L. Bianchini,[23] M. Bianco,[30] O. Biebel,[100] D. Biedermann,[16] S. P. Bieniek,[78] N. V. Biesuz,[124a,124b] M. Biglietti,[134a] J. Bilbao De Mendizabal,[49] H. Bilokon,[47] M. Bindi,[54] S. Binet,[117] A. Bingul,[19b] C. Bini,[132a,132b] S. Biondi,[20a,20b] D. M. Bjergaard,[45] C. W. Black,[150] J. E. Black,[143] K. M. Black,[22] D. Blackburn,[138] R. E. Blair,[6] J.-B. Blanchard,[136] J. E. Blanco,[77] T. Blazek,[144a] I. Bloch,[42] C. Blocker,[23] W. Blum,[83,a] U. Blumenschein,[54] S. Blunier,[32a] G. J. Bobbink,[107] V. S. Bobrovnikov,[109,d] S. S. Bocchetta,[81] A. Bocci,[45] C. Bock,[100] M. Boehler,[48] J. A. Bogaerts,[30] D. Bogavac,[13] A. G. Bogdanchikov,[109] C. Bohm,[146a] V. Boisvert,[77] T. Bold,[38a] V. Boldea,[26b] A. S. Boldyrev,[99] M. Bomben,[80] M. Bona,[76] M. Boonekamp,[136] A. Borisov,[130] G. Borissov,[72] S. Borroni,[42] J. Bortfeldt,[100] V. Bortolotto,[60a,60b,60c] K. Bos,[107] D. Boscherini,[20a] M. Bosman,[12] J. Boudreau,[125] J. Bouffard,[2] E. V. Bouhova-Thacker,[72] D. Boumediene,[34] C. Bourdarios,[117] N. Bousson,[114] S. K. Boutle,[53] A. Boveia,[30] J. Boyd,[30] I. R. Boyko,[65] I. Bozic,[13] J. Bracinik,[18] A. Brandt,[8] G. Brandt,[54] O. Brandt,[58a] U. Bratzler,[156] B. Brau,[86] J. E. Brau,[116] H. M. Braun,[175,a] W. D. Breaden Madden,[53] K. Brendlinger,[122] A. J. Brennan,[88] L. Brenner,[107] R. Brenner,[166] S. Bressler,[172] T. M. Bristow,[46] D. Britton,[53] D. Britzger,[42] F. M. Brochu,[28] I. Brock,[21] R. Brock,[90] J. Bronner,[101] G. Brooijmans,[35] T. Brooks,[77] W. K. Brooks,[32b] J. Brosamer,[15] E. Brost,[116] P. A. Bruckman de Renstrom,[39] D. Bruncko,[144b] R. Bruneliere,[48] A. Bruni,[20a] G. Bruni,[20a] M. Bruschi,[20a] N. Bruscino,[21] L. Bryngemark,[81] T. Buanes,[14] Q. Buat,[142] P. Buchholz,[141] A. G. Buckley,[53] S. I. Buda,[26b] I. A. Budagov,[65] F. Buehrer,[48] L. Bugge,[119] M. K. Bugge,[119] O. Bulekov,[98] D. Bullock,[8] H. Burckhart,[30] S. Burdin,[74] C. D. Burgard,[48] B. Burghgrave,[108] S. Burke,[131] I. Burmeister,[43] E. Busato,[34] D. Büscher,[48] V. Büscher,[83] P. Bussey,[53] J. M. Butler,[22] A. I. Butt,[3] C. M. Buttar,[53] J. M. Butterworth,[78] P. Butti,[107] W. Buttinger,[25] A. Buzatu,[53] A. R. Buzykaev,[109,d] S. Cabrera Urbán,[167] D. Caforio,[128] V. M. Cairo,[37a,37b] O. Cakir,[4a] N. Calace,[49] P. Calafiura,[15] A. Calandri,[136] G. Calderini,[80] P. Calfayan,[100] L. P. Caloba,[24a] D. Calvet,[34] S. Calvet,[34] R. Camacho Toro,[31] S. Camarda,[42] P. Camarri,[133a,133b] D. Cameron,[119] R. Caminal Armadans,[165] S. Campana,[30] M. Campanelli,[78] A. Campoverde,[148] V. Canale,[104a,104b] A. Canepa,[159a] M. Cano Bret,[33e] J. Cantero,[82] R. Cantrill,[126a] T. Cao,[40] M. D. M. Capeans Garrido,[30] I. Caprini,[26b] M. Caprini,[26b] M. Capua,[37a,37b] R. Caputo,[83] R. M. Carbone,[35] R. Cardarelli,[133a] F. Cardillo,[48] T. Carli,[30] G. Carlino,[104a] L. Carminati,[91a,91b] S. Caron,[106] E. Carquin,[32a] G. D. Carrillo-Montoya,[30] J. R. Carter,[28] J. Carvalho,[126a,126c] D. Casadei,[78] M. P. Casado,[12] M. Casolino,[12] E. Castaneda-Miranda,[145a] A. Castelli,[107] V. Castillo Gimenez,[167] N. F. Castro,[126a,h] P. Catastini,[57] A. Catinaccio,[30] J. R. Catmore,[119] A. Cattai,[30] J. Caudron,[83] V. Cavaliere,[165] D. Cavalli,[91a] M. Cavalli-Sforza,[12] V. Cavasinni,[124a,124b] F. Ceradini,[134a,134b] B. C. Cerio,[45] K. Cerny,[129] A. S. Cerqueira,[24b] A. Cerri,[149] L. Cerrito,[76] F. Cerutti,[15] M. Cerv,[30] A. Cervelli,[17] S. A. Cetin,[19c] A. Chafaq,[135a] D. Chakraborty,[108] I. Chalupkova,[129] Y. L. Chan,[60a] P. Chang,[165] J. D. Chapman,[28] D. G. Charlton,[18] C. C. Chau,[158] C. A. Chavez Barajas,[149] S. Cheatham,[152] A. Chegwidden,[90] S. Chekanov,[6] S. V. Chekulaev,[159a] G. A. Chelkov,[65,i] M. A. Chelstowska,[89] C. Chen,[64] H. Chen,[25] K. Chen,[148] L. Chen,[33d,j] S. Chen,[33c] S. Chen,[155] X. Chen,[33f] Y. Chen,[67] H. C. Cheng,[89] Y. Cheng,[31] A. Cheplakov,[65] E. Cheremushkina,[130] R. Cherkaoui El Moursli,[135e] V. Chernyatin,[25,a] E. Cheu,[7] L. Chevalier,[136] V. Chiarella,[47] G. Chiarelli,[124a,124b] G. Chiodini,[73a] A. S. Chisholm,[18] R. T. Chislett,[78] A. Chitan,[26b] M. V. Chizhov,[65] K. Choi,[61] S. Chouridou,[9] B. K. B. Chow,[100] V. Christodoulou,[78] D. Chromek-Burckhart,[30] J. Chudoba,[127] A. J. Chuinard,[87]

J. J. Chwastowski,[39] L. Chytka,[115] G. Ciapetti,[132a,132b] A. K. Ciftci,[4a] D. Cinca,[53] V. Cindro,[75] I. A. Cioara,[21] A. Ciocio,[15] F. Cirotto,[104a,104b] Z. H. Citron,[172] M. Ciubancan,[26b] A. Clark,[49] B. L. Clark,[57] P. J. Clark,[46] R. N. Clarke,[15] C. Clement,[146a,146b] Y. Coadou,[85] M. Cobal,[164a,164c] A. Coccaro,[49] J. Cochran,[64] L. Coffey,[23] J. G. Cogan,[143] L. Colasurdo,[106] B. Cole,[35] S. Cole,[108] A. P. Colijn,[107] J. Collot,[55] T. Colombo,[58c] G. Compostella,[101] P. Conde Muiño,[126a,126b] E. Coniavitis,[48] S. H. Connell,[145b] I. A. Connelly,[77] V. Consorti,[48] S. Constantinescu,[26b] C. Conta,[121a,121b] G. Conti,[30] F. Conventi,[104a,k] M. Cooke,[15] B. D. Cooper,[78] A. M. Cooper-Sarkar,[120] T. Cornelissen,[175] M. Corradi,[20a] F. Corriveau,[87,l] A. Corso-Radu,[163] A. Cortes-Gonzalez,[12] G. Cortiana,[101] G. Costa,[91a] M. J. Costa,[167] D. Costanzo,[139] D. Côté,[8] G. Cottin,[28] G. Cowan,[77] B. E. Cox,[84] K. Cranmer,[110] G. Cree,[29] S. Crépé-Renaudin,[55] F. Crescioli,[80] W. A. Cribbs,[146a,146b] M. Crispin Ortuzar,[120] M. Cristinziani,[21] V. Croft,[106] G. Crosetti,[37a,37b] T. Cuhadar Donszelmann,[139] J. Cummings,[176] M. Curatolo,[47] J. Cúth,[83] C. Cuthbert,[150] H. Czirr,[141] P. Czodrowski,[3] S. D'Auria,[53] M. D'Onofrio,[74] M. J. Da Cunha Sargedas De Sousa,[126a,126b] C. Da Via,[84] W. Dabrowski,[38a] A. Dafinca,[120] T. Dai,[89] O. Dale,[14] F. Dallaire,[95] C. Dallapiccola,[86] M. Dam,[36] J. R. Dandoy,[31] N. P. Dang,[48] A. C. Daniells,[18] M. Danninger,[168] M. Dano Hoffmann,[136] V. Dao,[48] G. Darbo,[50a] S. Darmora,[8] J. Dassoulas,[3] A. Dattagupta,[61] W. Davey,[21] C. David,[169] T. Davidek,[129] E. Davies,[120,m] M. Davies,[153] P. Davison,[78] Y. Davygora,[58a] E. Dawe,[88] I. Dawson,[139] R. K. Daya-Ishmukhametova,[86] K. De,[8] R. de Asmundis,[104a] A. De Benedetti,[113] S. De Castro,[20a,20b] S. De Cecco,[80] N. De Groot,[106] P. de Jong,[107] H. De la Torre,[82] F. De Lorenzi,[64] D. De Pedis,[132a] A. De Salvo,[132a] U. De Sanctis,[149] A. De Santo,[149] J. B. De Vivie De Regie,[117] W. J. Dearnaley,[72] R. Debbe,[25] C. Debenedetti,[137] D. V. Dedovich,[65] I. Deigaard,[107] J. Del Peso,[82] T. Del Prete,[124a,124b] D. Delgove,[117] F. Deliot,[136] C. M. Delitzsch,[49] M. Deliyergiyev,[75] A. Dell'Acqua,[30] L. Dell'Asta,[22] M. Dell'Orso,[124a,124b] M. Della Pietra,[104a,k] D. della Volpe,[49] M. Delmastro,[5] P. A. Delsart,[55] C. Deluca,[107] D. A. DeMarco,[158] S. Demers,[176] M. Demichev,[65] A. Demilly,[80] S. P. Denisov,[130] D. Derendarz,[39] J. E. Derkaoui,[135d] F. Derue,[80] P. Dervan,[74] K. Desch,[21] C. Deterre,[42] K. Dette,[43] P. O. Deviveiros,[30] A. Dewhurst,[131] S. Dhaliwal,[23] A. Di Ciaccio,[133a,133b] L. Di Ciaccio,[5] A. Di Domenico,[132a,132b] C. Di Donato,[132a,132b] A. Di Girolamo,[30] B. Di Girolamo,[30] A. Di Mattia,[152] B. Di Micco,[134a,134b] R. Di Nardo,[47] A. Di Simone,[48] R. Di Sipio,[158] D. Di Valentino,[29] C. Diaconu,[85] M. Diamond,[158] F. A. Dias,[46] M. A. Diaz,[32a] E. B. Diehl,[89] J. Dietrich,[16] S. Diglio,[85] A. Dimitrievska,[13] J. Dingfelder,[21] P. Dita,[26b] S. Dita,[26b] F. Dittus,[30] F. Djama,[85] T. Djobava,[51b] J. I. Djuvsland,[58a] M. A. B. do Vale,[24c] D. Dobos,[30] M. Dobre,[26b] C. Doglioni,[81] T. Dohmae,[155] J. Dolejsi,[129] Z. Dolezal,[129] B. A. Dolgoshein,[98,a] M. Donadelli,[24d] S. Donati,[124a,124b] P. Dondero,[121a,121b] J. Donini,[34] J. Dopke,[131] A. Doria,[104a] M. T. Dova,[71] A. T. Doyle,[53] E. Drechsler,[54] M. Dris,[10] E. Dubreuil,[34] E. Duchovni,[172] G. Duckeck,[100] O. A. Ducu,[26b,85] D. Duda,[107] A. Dudarev,[30] L. Duflot,[117] L. Duguid,[77] M. Dührssen,[30] M. Dunford,[58a] H. Duran Yildiz,[4a] M. Düren,[52] A. Durglishvili,[51b] D. Duschinger,[44] B. Dutta,[42] M. Dyndal,[38a] C. Eckardt,[42] K. M. Ecker,[101] R. C. Edgar,[89] W. Edson,[2] N. C. Edwards,[46] W. Ehrenfeld,[21] T. Eifert,[30] G. Eigen,[14] K. Einsweiler,[15] T. Ekelof,[166] M. El Kacimi,[135c] M. Ellert,[166] S. Elles,[5] F. Ellinghaus,[175] A. A. Elliot,[169] N. Ellis,[30] J. Elmsheuser,[100] M. Elsing,[30] D. Emeliyanov,[131] Y. Enari,[155] O. C. Endner,[83] M. Endo,[118] J. Erdmann,[43] A. Ereditato,[17] G. Ernis,[175] J. Ernst,[2] M. Ernst,[25] S. Errede,[165] E. Ertel,[83] M. Escalier,[117] H. Esch,[43] C. Escobar,[125] B. Esposito,[47] A. I. Etienvre,[136] E. Etzion,[153] H. Evans,[61] A. Ezhilov,[123] L. Fabbri,[20a,20b] G. Facini,[31] R. M. Fakhrutdinov,[130] S. Falciano,[132a] R. J. Falla,[78] J. Faltova,[129] Y. Fang,[33a] M. Fanti,[91a,91b] A. Farbin,[8] A. Farilla,[134a] T. Farooque,[12] S. Farrell,[15] S. M. Farrington,[170] P. Farthouat,[30] F. Fassi,[135e] P. Fassnacht,[30] D. Fassouliotis,[9] M. Faucci Giannelli,[77] A. Favareto,[50a,50b] L. Fayard,[117] O. L. Fedin,[123,n] W. Fedorko,[168] S. Feigl,[30] L. Feligioni,[85] C. Feng,[33d] E. J. Feng,[30] H. Feng,[89] A. B. Fenyuk,[130] L. Feremenga,[8] P. Fernandez Martinez,[167] S. Fernandez Perez,[30] J. Ferrando,[53] A. Ferrari,[166] P. Ferrari,[107] R. Ferrari,[121a] D. E. Ferreira de Lima,[53] A. Ferrer,[167] D. Ferrere,[49] C. Ferretti,[89] A. Ferretto Parodi,[50a,50b] M. Fiascaris,[31] F. Fiedler,[83] A. Filipčič,[75] M. Filipuzzi,[42] F. Filthaut,[106] M. Fincke-Keeler,[169] K. D. Finelli,[150] M. C. N. Fiolhais,[126a,126c] L. Fiorini,[167] A. Firan,[40] A. Fischer,[2] C. Fischer,[12] J. Fischer,[175] W. C. Fisher,[90] N. Flaschel,[42] I. Fleck,[141] P. Fleischmann,[89] G. T. Fletcher,[139] G. Fletcher,[76] R. R. M. Fletcher,[122] T. Flick,[175] A. Floderus,[81] L. R. Flores Castillo,[60a] M. J. Flowerdew,[101] A. Formica,[136] A. Forti,[84] D. Fournier,[117] H. Fox,[72] S. Fracchia,[12] P. Francavilla,[80] M. Franchini,[20a,20b] D. Francis,[30] L. Franconi,[119] M. Franklin,[57] M. Frate,[163] M. Fraternali,[121a,121b] D. Freeborn,[78] S. T. French,[28] F. Friedrich,[44] D. Froidevaux,[30] J. A. Frost,[120] R. Fuchi,[160] C. Fukunaga,[156] E. Fullana Torregrosa,[83] B. G. Fulsom,[143] T. Fusayasu,[102] J. Fuster,[167] C. Gabaldon,[55] O. Gabizon,[175] A. Gabrielli,[20a,20b] A. Gabrielli,[15] G. P. Gach,[18] S. Gadatsch,[30] S. Gadomski,[49] G. Gagliardi,[50a,50b] P. Gagnon,[61] C. Galea,[106] B. Galhardo,[126a,126c] E. J. Gallas,[120] B. J. Gallop,[131] P. Gallus,[128] G. Galster,[36] K. K. Gan,[111] J. Gao,[33b,85] Y. Gao,[46] Y. S. Gao,[143,f] F. M. Garay Walls,[46] F. Garberson,[176] C. García,[167] J. E. García Navarro,[167] M. Garcia-Sciveres,[15] R. W. Gardner,[31] N. Garelli,[143] V. Garonne,[119] C. Gatti,[47] A. Gaudiello,[50a,50b] G. Gaudio,[121a] B. Gaur,[141] L. Gauthier,[95]

P. Gauzzi,[132a,132b] I. L. Gavrilenko,[96] C. Gay,[168] G. Gaycken,[21] E. N. Gazis,[10] P. Ge,[33d] Z. Gecse,[168] C. N. P. Gee,[131] Ch. Geich-Gimbel,[21] M. P. Geisler,[58a] C. Gemme,[50a] M. H. Genest,[55] S. Gentile,[132a,132b] M. George,[54] S. George,[77] D. Gerbaudo,[163] A. Gershon,[153] S. Ghasemi,[141] H. Ghazlane,[135b] B. Giacobbe,[20a] S. Giagu,[132a,132b] V. Giangiobbe,[12] P. Giannetti,[124a,124b] B. Gibbard,[25] S. M. Gibson,[77] M. Gignac,[168] M. Gilchriese,[15] T. P. S. Gillam,[28] D. Gillberg,[30] G. Gilles,[34] D. M. Gingrich,[3,e] N. Giokaris,[9] M. P. Giordani,[164a,164c] F. M. Giorgi,[20a] F. M. Giorgi,[16] P. F. Giraud,[136] P. Giromini,[47] D. Giugni,[91a] C. Giuliani,[101] M. Giulini,[58b] B. K. Gjelsten,[119] S. Gkaitatzis,[154] I. Gkialas,[154] E. L. Gkougkousis,[117] L. K. Gladilin,[99] C. Glasman,[82] J. Glatzer,[30] P. C. F. Glaysher,[46] A. Glazov,[42] M. Goblirsch-Kolb,[101] J. R. Goddard,[76] J. Godlewski,[39] S. Goldfarb,[89] T. Golling,[49] D. Golubkov,[130] A. Gomes,[126a,126b,126d] R. Gonçalo,[126a] J. Goncalves Pinto Firmino Da Costa,[136] L. Gonella,[21] S. González de la Hoz,[167] G. Gonzalez Parra,[12] S. Gonzalez-Sevilla,[49] L. Goossens,[30] P. A. Gorbounov,[97] H. A. Gordon,[25] I. Gorelov,[105] B. Gorini,[30] E. Gorini,[73a,73b] A. Gorišek,[75] E. Gornicki,[39] A. T. Goshaw,[45] C. Gössling,[43] M. I. Gostkin,[65] D. Goujdami,[135c] A. G. Goussiou,[138] N. Govender,[145b] E. Gozani,[152] H. M. X. Grabas,[137] L. Graber,[54] I. Grabowska-Bold,[38a] P. O. J. Gradin,[166] P. Grafström,[20a,20b] J. Gramling,[49] E. Gramstad,[119] S. Grancagnolo,[16] V. Gratchev,[123] H. M. Gray,[30] E. Graziani,[134a] Z. D. Greenwood,[79,o] C. Grefe,[21] K. Gregersen,[78] I. M. Gregor,[42] P. Grenier,[143] J. Griffiths,[8] A. A. Grillo,[137] K. Grimm,[72] S. Grinstein,[12,p] Ph. Gris,[34] J.-F. Grivaz,[117] J. P. Grohs,[44] A. Grohsjean,[42] E. Gross,[172] J. Grosse-Knetter,[54] G. C. Grossi,[79] Z. J. Grout,[149] L. Guan,[89] J. Guenther,[128] F. Guescini,[49] D. Guest,[163] O. Gueta,[153] E. Guido,[50a,50b] T. Guillemin,[117] S. Guindon,[2] U. Gul,[53] C. Gumpert,[44] J. Guo,[33e] Y. Guo,[33b,q] S. Gupta,[120] G. Gustavino,[132a,132b] P. Gutierrez,[113] N. G. Gutierrez Ortiz,[78] C. Gutschow,[44] C. Guyot,[136] C. Gwenlan,[120] C. B. Gwilliam,[74] A. Haas,[110] C. Haber,[15] H. K. Hadavand,[8] N. Haddad,[135e] P. Haefner,[21] S. Hageböck,[21] Z. Hajduk,[39] H. Hakobyan,[177] M. Haleem,[42] J. Haley,[114] D. Hall,[120] G. Halladjian,[90] G. D. Hallewell,[85] K. Hamacher,[175] P. Hamal,[115] K. Hamano,[169] A. Hamilton,[145a] G. N. Hamity,[139] P. G. Hamnett,[42] L. Han,[33b] K. Hanagaki,[66,r] K. Hanawa,[155] M. Hance,[137] B. Haney,[122] P. Hanke,[58a] R. Hanna,[136] J. B. Hansen,[36] J. D. Hansen,[36] M. C. Hansen,[21] P. H. Hansen,[36] K. Hara,[160] A. S. Hard,[173] T. Harenberg,[175] F. Hariri,[117] S. Harkusha,[92] R. D. Harrington,[46] P. F. Harrison,[170] F. Hartjes,[107] M. Hasegawa,[67] Y. Hasegawa,[140] A. Hasib,[113] S. Hassani,[136] S. Haug,[17] R. Hauser,[90] L. Hauswald,[44] M. Havranek,[127] C. M. Hawkes,[18] R. J. Hawkings,[30] A. D. Hawkins,[81] T. Hayashi,[160] D. Hayden,[90] C. P. Hays,[120] J. M. Hays,[76] H. S. Hayward,[74] S. J. Haywood,[131] S. J. Head,[18] T. Heck,[83] V. Hedberg,[81] L. Heelan,[8] S. Heim,[122] T. Heim,[175] B. Heinemann,[15] L. Heinrich,[110] J. Hejbal,[127] L. Helary,[22] S. Hellman,[146a,146b] D. Hellmich,[21] C. Helsens,[12] J. Henderson,[120] R. C. W. Henderson,[72] Y. Heng,[173] C. Hengler,[42] S. Henkelmann,[168] A. Henrichs,[176] A. M. Henriques Correia,[30] S. Henrot-Versille,[117] G. H. Herbert,[16] Y. Hernández Jiménez,[167] G. Herten,[48] R. Hertenberger,[100] L. Hervas,[30] G. G. Hesketh,[78] N. P. Hessey,[107] J. W. Hetherly,[40] R. Hickling,[76] E. Higón-Rodriguez,[167] E. Hill,[169] J. C. Hill,[28] K. H. Hiller,[42] S. J. Hillier,[18] I. Hinchliffe,[15] E. Hines,[122] R. R. Hinman,[15] M. Hirose,[157] D. Hirschbuehl,[175] J. Hobbs,[148] N. Hod,[107] M. C. Hodgkinson,[139] P. Hodgson,[139] A. Hoecker,[30] M. R. Hoeferkamp,[105] F. Hoenig,[100] M. Hohlfeld,[83] D. Hohn,[21] T. R. Holmes,[15] M. Homann,[43] T. M. Hong,[125] W. H. Hopkins,[116] Y. Horii,[103] A. J. Horton,[142] J-Y. Hostachy,[55] S. Hou,[151] A. Hoummada,[135a] J. Howard,[120] J. Howarth,[42] M. Hrabovsky,[115] I. Hristova,[16] J. Hrivnac,[117] T. Hryn'ova,[5] A. Hrynevich,[93] C. Hsu,[145c] P. J. Hsu,[151,s] S.-C. Hsu,[138] D. Hu,[35] Q. Hu,[33b] X. Hu,[89] Y. Huang,[42] Z. Hubacek,[128] F. Hubaut,[85] F. Huegging,[21] T. B. Huffman,[120] E. W. Hughes,[35] G. Hughes,[72] M. Huhtinen,[30] T. A. Hülsing,[83] N. Huseynov,[65,c] J. Huston,[90] J. Huth,[57] G. Iacobucci,[49] G. Iakovidis,[25] I. Ibragimov,[141] L. Iconomidou-Fayard,[117] E. Ideal,[176] Z. Idrissi,[135e] P. Iengo,[30] O. Igonkina,[107] T. Iizawa,[171] Y. Ikegami,[66] K. Ikematsu,[141] M. Ikeno,[66] Y. Ilchenko,[31,t] D. Iliadis,[154] N. Ilic,[143] T. Ince,[101] G. Introzzi,[121a,121b] P. Ioannou,[9] M. Iodice,[134a] K. Iordanidou,[35] V. Ippolito,[57] A. Irles Quiles,[167] C. Isaksson,[166] M. Ishino,[68] M. Ishitsuka,[157] R. Ishmukhametov,[111] C. Issever,[120] S. Istin,[19a] J. M. Iturbe Ponce,[84] R. Iuppa,[133a,133b] J. Ivarsson,[81] W. Iwanski,[39] H. Iwasaki,[66] J. M. Izen,[41] V. Izzo,[104a] S. Jabbar,[3] B. Jackson,[122] M. Jackson,[74] P. Jackson,[1] M. R. Jaekel,[30] V. Jain,[2] K. Jakobs,[48] S. Jakobsen,[30] T. Jakoubek,[127] J. Jakubek,[128] D. O. Jamin,[114] D. K. Jana,[79] E. Jansen,[78] R. Jansky,[62] J. Janssen,[21] M. Janus,[54] G. Jarlskog,[81] N. Javadov,[65,c] T. Javůrek,[48] L. Jeanty,[15] J. Jejelava,[51a,u] G.-Y. Jeng,[150] D. Jennens,[88] P. Jenni,[48,v] J. Jentzsch,[43] C. Jeske,[170] S. Jézéquel,[5] H. Ji,[173] J. Jia,[148] Y. Jiang,[33b] S. Jiggins,[78] J. Jimenez Pena,[167] S. Jin,[33a] A. Jinaru,[26b] O. Jinnouchi,[157] M. D. Joergensen,[36] P. Johansson,[139] K. A. Johns,[7] W. J. Johnson,[138] K. Jon-And,[146a,146b] G. Jones,[170] R. W. L. Jones,[72] T. J. Jones,[74] J. Jongmanns,[58a] P. M. Jorge,[126a,126b] K. D. Joshi,[84] J. Jovicevic,[159a] X. Ju,[173] P. Jussel,[62] A. Juste Rozas,[12,p] M. Kaci,[167] A. Kaczmarska,[39] M. Kado,[117] H. Kagan,[111] M. Kagan,[143] S. J. Kahn,[85] E. Kajomovitz,[45] C. W. Kalderon,[120] S. Kama,[40] A. Kamenshchikov,[130] N. Kanaya,[155] S. Kaneti,[28] V. A. Kantserov,[98] J. Kanzaki,[66] B. Kaplan,[110] L. S. Kaplan,[173] A. Kapliy,[31] D. Kar,[145c] K. Karakostas,[10] A. Karamaoun,[3] N. Karastathis,[10,107] M. J. Kareem,[54] E. Karentzos,[10] M. Karnevskiy,[83] S. N. Karpov,[65]

Z. M. Karpova,[65] K. Karthik,[110] V. Kartvelishvili,[72] A. N. Karyukhin,[130] K. Kasahara,[160] L. Kashif,[173] R. D. Kass,[111] A. Kastanas,[14] Y. Kataoka,[155] C. Kato,[155] A. Katre,[49] J. Katzy,[42] K. Kawade,[103] K. Kawagoe,[70] T. Kawamoto,[155] G. Kawamura,[54] S. Kazama,[155] V. F. Kazanin,[109,d] R. Keeler,[169] R. Kehoe,[40] J. S. Keller,[42] J. J. Kempster,[77] H. Keoshkerian,[84] O. Kepka,[127] B. P. Kerševan,[75] S. Kersten,[175] R. A. Keyes,[87] F. Khalil-zada,[11] H. Khandanyan,[146a,146b] A. Khanov,[114] A. G. Kharlamov,[109,d] T. J. Khoo,[28] V. Khovanskiy,[97] E. Khramov,[65] J. Khubua,[51b,w] S. Kido,[67] H. Y. Kim,[8] S. H. Kim,[160] Y. K. Kim,[31] N. Kimura,[154] O. M. Kind,[16] B. T. King,[74] M. King,[167] S. B. King,[168] J. Kirk,[131] A. E. Kiryunin,[101] T. Kishimoto,[67] D. Kisielewska,[38a] F. Kiss,[48] K. Kiuchi,[160] O. Kivernyk,[136] E. Kladiva,[144b] M. H. Klein,[35] M. Klein,[74] U. Klein,[74] K. Kleinknecht,[83] P. Klimek,[146a,146b] A. Klimentov,[25] R. Klingenberg,[43] J. A. Klinger,[139] T. Klioutchnikova,[30] E.-E. Kluge,[58a] P. Kluit,[107] S. Kluth,[101] J. Knapik,[39] E. Kneringer,[62] E. B. F. G. Knoops,[85] A. Knue,[53] A. Kobayashi,[155] D. Kobayashi,[157] T. Kobayashi,[155] M. Kobel,[44] M. Kocian,[143] P. Kodys,[129] T. Koffas,[29] E. Koffeman,[107] L. A. Kogan,[120] S. Kohlmann,[175] Z. Kohout,[128] T. Kohriki,[66] T. Koi,[143] H. Kolanoski,[16] M. Kolb,[58b] I. Koletsou,[5] A. A. Komar,[96,a] Y. Komori,[155] T. Kondo,[66] N. Kondrashova,[42] K. Köneke,[48] A. C. König,[106] T. Kono,[66] R. Konoplich,[110,x] N. Konstantinidis,[78] R. Kopeliansky,[152] S. Koperny,[38a] L. Köpke,[83] A. K. Kopp,[48] K. Korcyl,[39] K. Kordas,[154] A. Korn,[78] A. A. Korol,[109,d] I. Korolkov,[12] E. V. Korolkova,[139] O. Kortner,[101] S. Kortner,[101] T. Kosek,[129] V. V. Kostyukhin,[21] V. M. Kotov,[65] A. Kotwal,[45] A. Kourkoumeli-Charalampidi,[154] C. Kourkoumelis,[9] V. Kouskoura,[25] A. Koutsman,[159a] R. Kowalewski,[169] T. Z. Kowalski,[38a] W. Kozanecki,[136] A. S. Kozhin,[130] V. A. Kramarenko,[99] G. Kramberger,[75] D. Krasnopevtsev,[98] M. W. Krasny,[80] A. Krasznahorkay,[30] J. K. Kraus,[21] A. Kravchenko,[25] S. Kreiss,[110] M. Kretz,[58c] J. Kretzschmar,[74] K. Kreutzfeldt,[52] P. Krieger,[158] K. Krizka,[31] K. Kroeninger,[43] H. Kroha,[101] J. Kroll,[122] J. Kroseberg,[21] J. Krstic,[13] U. Kruchonak,[65] H. Krüger,[21] N. Krumnack,[64] A. Kruse,[173] M. C. Kruse,[45] M. Kruskal,[22] T. Kubota,[88] H. Kucuk,[78] S. Kuday,[4b] S. Kuehn,[48] A. Kugel,[58c] F. Kuger,[174] A. Kuhl,[137] T. Kuhl,[42] V. Kukhtin,[65] R. Kukla,[136] Y. Kulchitsky,[92] S. Kuleshov,[32b] M. Kuna,[132a,132b] T. Kunigo,[68] A. Kupco,[127] H. Kurashige,[67] Y. A. Kurochkin,[92] V. Kus,[127] E. S. Kuwertz,[169] M. Kuze,[157] J. Kvita,[115] T. Kwan,[169] D. Kyriazopoulos,[139] A. La Rosa,[137] J. L. La Rosa Navarro,[24d] L. La Rotonda,[37a,37b] C. Lacasta,[167] F. Lacava,[132a,132b] J. Lacey,[29] H. Lacker,[16] D. Lacour,[80] V. R. Lacuesta,[167] E. Ladygin,[65] R. Lafaye,[5] B. Laforge,[80] T. Lagouri,[176] S. Lai,[54] L. Lambourne,[78] S. Lammers,[61] C. L. Lampen,[7] W. Lampl,[7] E. Lançon,[136] U. Landgraf,[48] M. P. J. Landon,[76] V. S. Lang,[58a] J. C. Lange,[12] A. J. Lankford,[163] F. Lanni,[25] K. Lantzsch,[21] A. Lanza,[121a] S. Laplace,[80] C. Lapoire,[30] J. F. Laporte,[136] T. Lari,[91a] F. Lasagni Manghi,[20a,20b] M. Lassnig,[30] P. Laurelli,[47] W. Lavrijsen,[15] A. T. Law,[137] P. Laycock,[74] T. Lazovich,[57] O. Le Dortz,[80] E. Le Guirriec,[85] E. Le Menedeu,[12] M. LeBlanc,[169] T. LeCompte,[6] F. Ledroit-Guillon,[55] C. A. Lee,[145a] S. C. Lee,[151] L. Lee,[1] G. Lefebvre,[80] M. Lefebvre,[169] F. Legger,[100] C. Leggett,[15] A. Lehan,[74] G. Lehmann Miotto,[30] X. Lei,[7] W. A. Leight,[29] A. Leisos,[154,y] A. G. Leister,[176] M. A. L. Leite,[24d] R. Leitner,[129] D. Lellouch,[172] B. Lemmer,[54] K. J. C. Leney,[78] T. Lenz,[21] B. Lenzi,[30] R. Leone,[7] S. Leone,[124a,124b] C. Leonidopoulos,[46] S. Leontsinis,[10] C. Leroy,[95] C. G. Lester,[28] M. Levchenko,[123] J. Levêque,[5] D. Levin,[89] L. J. Levinson,[172] M. Levy,[18] A. Lewis,[120] A. M. Leyko,[21] M. Leyton,[41] B. Li,[33b,z] H. Li,[148] H. L. Li,[31] L. Li,[45] L. Li,[33e] S. Li,[45] X. Li,[84] Y. Li,[33c,aa] Z. Liang,[137] H. Liao,[34] B. Liberti,[133a] A. Liblong,[158] P. Lichard,[30] K. Lie,[165] J. Liebal,[21] W. Liebig,[14] C. Limbach,[21] A. Limosani,[150] S. C. Lin,[151,bb] T. H. Lin,[83] F. Linde,[107] B. E. Lindquist,[148] J. T. Linnemann,[90] E. Lipeles,[122] A. Lipniacka,[14] M. Lisovyi,[58b] T. M. Liss,[165] D. Lissauer,[25] A. Lister,[168] A. M. Litke,[137] B. Liu,[151,cc] D. Liu,[151] H. Liu,[89] J. Liu,[85] J. B. Liu,[33b] K. Liu,[85] L. Liu,[165] M. Liu,[45] M. Liu,[33b] Y. Liu,[33b] M. Livan,[121a,121b] A. Lleres,[55] J. Llorente Merino,[82] S. L. Lloyd,[76] F. Lo Sterzo,[151] E. Lobodzinska,[42] P. Loch,[7] W. S. Lockman,[137] F. K. Loebinger,[84] A. E. Loevschall-Jensen,[36] K. M. Loew,[23] A. Loginov,[176] T. Lohse,[16] K. Lohwasser,[42] M. Lokajicek,[127] B. A. Long,[22] J. D. Long,[165] R. E. Long,[72] K. A. Looper,[111] L. Lopes,[126a] D. Lopez Mateos,[57] B. Lopez Paredes,[139] I. Lopez Paz,[12] J. Lorenz,[100] N. Lorenzo Martinez,[61] M. Losada,[162] P. J. Lösel,[100] X. Lou,[33a] A. Lounis,[117] J. Love,[6] P. A. Love,[72] H. Lu,[60a] N. Lu,[89] H. J. Lubatti,[138] C. Luci,[132a,132b] A. Lucotte,[55] C. Luedtke,[48] F. Luehring,[61] W. Lukas,[62] L. Luminari,[132a] O. Lundberg,[146a,146b] B. Lund-Jensen,[147] D. Lynn,[25] R. Lysak,[127] E. Lytken,[81] H. Ma,[25] L. L. Ma,[33d] G. Maccarrone,[47] A. Macchiolo,[101] C. M. Macdonald,[139] B. Maček,[75] J. Machado Miguens,[122,126b] D. Macina,[30] D. Madaffari,[85] R. Madar,[34] H. J. Maddocks,[72] W. F. Mader,[44] A. Madsen,[166] J. Maeda,[67] S. Maeland,[14] T. Maeno,[25] A. Maevskiy,[99] E. Magradze,[54] K. Mahboubi,[48] J. Mahlstedt,[107] C. Maiani,[136] C. Maidantchik,[24a] A. A. Maier,[101] T. Maier,[100] A. Maio,[126a,126b,126d] S. Majewski,[116] Y. Makida,[66] N. Makovec,[117] B. Malaescu,[80] Pa. Malecki,[39] V. P. Maleev,[123] F. Malek,[55] U. Mallik,[63] D. Malon,[6] C. Malone,[143] S. Maltezos,[10] V. M. Malyshev,[109] S. Malyukov,[30] J. Mamuzic,[42] G. Mancini,[47] B. Mandelli,[30] L. Mandelli,[91a] I. Mandić,[75] R. Mandrysch,[63] J. Maneira,[126a,126b] A. Manfredini,[101] L. Manhaes de Andrade Filho,[24b] J. Manjarres Ramos,[159b] A. Mann,[100] A. Manousakis-Katsikakis,[9] B. Mansoulie,[136] R. Mantifel,[87] M. Mantoani,[54] L. Mapelli,[30] L. March,[145c] G. Marchiori,[80]

M. Marcisovsky,[127] C. P. Marino,[169] M. Marjanovic,[13] D. E. Marley,[89] F. Marroquim,[24a] S. P. Marsden,[84] Z. Marshall,[15] L. F. Marti,[17] S. Marti-Garcia,[167] B. Martin,[90] T. A. Martin,[170] V. J. Martin,[46] B. Martin dit Latour,[14] M. Martinez,[12,p] S. Martin-Haugh,[131] V. S. Martoiu,[26b] A. C. Martyniuk,[78] M. Marx,[138] F. Marzano,[132a] A. Marzin,[30] L. Masetti,[83] T. Mashimo,[155] R. Mashinistov,[96] J. Masik,[84] A. L. Maslennikov,[109,d] I. Massa,[20a,20b] L. Massa,[20a,20b] P. Mastrandrea,[5] A. Mastroberardino,[37a,37b] T. Masubuchi,[155] P. Mättig,[175] J. Mattmann,[83] J. Maurer,[26b] S. J. Maxfield,[74] D. A. Maximov,[109,d] R. Mazini,[151] S. M. Mazza,[91a,91b] G. Mc Goldrick,[158] S. P. Mc Kee,[89] A. McCarn,[89] R. L. McCarthy,[148] T. G. McCarthy,[29] N. A. McCubbin,[131] K. W. McFarlane,[56,a] J. A. Mcfayden,[78] G. Mchedlidze,[54] S. J. McMahon,[131] R. A. McPherson,[169,l] M. Medinnis,[42] S. Meehan,[145a] S. Mehlhase,[100] A. Mehta,[74] K. Meier,[58a] C. Meineck,[100] B. Meirose,[41] B. R. Mellado Garcia,[145c] F. Meloni,[17] A. Mengarelli,[20a,20b] S. Menke,[101] E. Meoni,[161] K. M. Mercurio,[57] S. Mergelmeyer,[21] P. Mermod,[49] L. Merola,[104a,104b] C. Meroni,[91a] F. S. Merritt,[31] A. Messina,[132a,132b] J. Metcalfe,[25] A. S. Mete,[163] C. Meyer,[83] C. Meyer,[122] J-P. Meyer,[136] J. Meyer,[107] H. Meyer Zu Theenhausen,[58a] R. P. Middleton,[131] S. Miglioranzi,[164a,164c] L. Mijović,[21] G. Mikenberg,[172] M. Mikestikova,[127] M. Mikuž,[75] M. Milesi,[88] A. Milic,[30] D. W. Miller,[31] C. Mills,[46] A. Milov,[172] D. A. Milstead,[146a,146b] A. A. Minaenko,[130] Y. Minami,[155] I. A. Minashvili,[65] A. I. Mincer,[110] B. Mindur,[38a] M. Mineev,[65] Y. Ming,[173] L. M. Mir,[12] K. P. Mistry,[122] T. Mitani,[171] J. Mitrevski,[100] V. A. Mitsou,[167] A. Miucci,[49] P. S. Miyagawa,[139] J. U. Mjörnmark,[81] T. Moa,[146a,146b] K. Mochizuki,[85] S. Mohapatra,[35] W. Mohr,[48] S. Molander,[146a,146b] R. Moles-Valls,[21] R. Monden,[68] K. Mönig,[42] C. Monini,[55] J. Monk,[36] E. Monnier,[85] A. Montalbano,[148] J. Montejo Berlingen,[12] F. Monticelli,[71] S. Monzani,[132a,132b] R. W. Moore,[3] N. Morange,[117] D. Moreno,[162] M. Moreno Llácer,[54] P. Morettini,[50a] D. Mori,[142] T. Mori,[155] M. Morii,[57] M. Morinaga,[155] V. Morisbak,[119] S. Moritz,[83] A. K. Morley,[150] G. Mornacchi,[30] J. D. Morris,[76] S. S. Mortensen,[36] A. Morton,[53] L. Morvaj,[103] M. Mosidze,[51b] J. Moss,[143] K. Motohashi,[157] R. Mount,[143] E. Mountricha,[25] S. V. Mouraviev,[96,a] E. J. W. Moyse,[86] S. Muanza,[85] R. D. Mudd,[18] F. Mueller,[101] J. Mueller,[125] R. S. P. Mueller,[100] T. Mueller,[28] D. Muenstermann,[49] P. Mullen,[53] G. A. Mullier,[17] J. A. Murillo Quijada,[18] W. J. Murray,[170,131] H. Musheghyan,[54] E. Musto,[152] A. G. Myagkov,[130,dd] M. Myska,[128] B. P. Nachman,[143] O. Nackenhorst,[54] J. Nadal,[54] K. Nagai,[120] R. Nagai,[157] Y. Nagai,[85] K. Nagano,[66] A. Nagarkar,[111] Y. Nagasaka,[59] K. Nagata,[160] M. Nagel,[101] E. Nagy,[85] A. M. Nairz,[30] Y. Nakahama,[30] K. Nakamura,[66] T. Nakamura,[155] I. Nakano,[112] H. Namasivayam,[41] R. F. Naranjo Garcia,[42] R. Narayan,[31] D. I. Narrias Villar,[58a] T. Naumann,[42] G. Navarro,[162] R. Nayyar,[7] H. A. Neal,[89] P. Yu. Nechaeva,[96] T. J. Neep,[84] P. D. Nef,[143] A. Negri,[121a,121b] M. Negrini,[20a] S. Nektarijevic,[106] C. Nellist,[117] A. Nelson,[163] S. Nemecek,[127] P. Nemethy,[110] A. A. Nepomuceno,[24a] M. Nessi,[30,ee] M. S. Neubauer,[165] M. Neumann,[175] R. M. Neves,[110] P. Nevski,[25] P. R. Newman,[18] D. H. Nguyen,[6] R. B. Nickerson,[120] R. Nicolaidou,[136] B. Nicquevert,[30] J. Nielsen,[137] N. Nikiforou,[35] A. Nikiforov,[16] V. Nikolaenko,[130,dd] I. Nikolic-Audit,[80] K. Nikolopoulos,[18] J. K. Nilsen,[119] P. Nilsson,[25] Y. Ninomiya,[155] A. Nisati,[132a] R. Nisius,[101] T. Nobe,[155] M. Nomachi,[118] I. Nomidis,[29] T. Nooney,[76] S. Norberg,[113] M. Nordberg,[30] O. Novgorodova,[44] S. Nowak,[101] M. Nozaki,[66] L. Nozka,[115] K. Ntekas,[10] G. Nunes Hanninger,[88] T. Nunnemann,[100] E. Nurse,[78] F. Nuti,[88] B. J. O'Brien,[46] F. O'grady,[7] D. C. O'Neil,[142] V. O'Shea,[53] F. G. Oakham,[29,e] H. Oberlack,[101] T. Obermann,[21] J. Ocariz,[80] A. Ochi,[67] I. Ochoa,[35] J. P. Ochoa-Ricoux,[32a] S. Oda,[70] S. Odaka,[66] H. Ogren,[61] A. Oh,[84] S. H. Oh,[45] C. C. Ohm,[15] H. Ohman,[166] H. Oide,[30] W. Okamura,[118] H. Okawa,[160] Y. Okumura,[31] T. Okuyama,[66] A. Olariu,[26b] S. A. Olivares Pino,[46] D. Oliveira Damazio,[25] A. Olszewski,[39] J. Olszowska,[39] A. Onofre,[126a,126e] K. Onogi,[103] P. U. E. Onyisi,[31,t] C. J. Oram,[159a] M. J. Oreglia,[31] Y. Oren,[153] D. Orestano,[134a,134b] N. Orlando,[154] C. Oropeza Barrera,[53] R. S. Orr,[158] B. Osculati,[50a,50b] R. Ospanov,[84] G. Otero y Garzon,[27] H. Otono,[70] M. Ouchrif,[135d] F. Ould-Saada,[119] A. Ouraou,[136] K. P. Oussoren,[107] Q. Ouyang,[33a] A. Ovcharova,[15] M. Owen,[53] R. E. Owen,[18] V. E. Ozcan,[19a] N. Ozturk,[8] K. Pachal,[142] A. Pacheco Pages,[12] C. Padilla Aranda,[12] M. Pagáčová,[48] S. Pagan Griso,[15] E. Paganis,[139] F. Paige,[25] P. Pais,[86] K. Pajchel,[119] G. Palacino,[159b] S. Palestini,[30] M. Palka,[38b] D. Pallin,[34] A. Palma,[126a,126b] Y. B. Pan,[173] E. St. Panagiotopoulou,[10] C. E. Pandini,[80] J. G. Panduro Vazquez,[77] P. Pani,[146a,146b] S. Panitkin,[25] D. Pantea,[26b] L. Paolozzi,[49] Th. D. Papadopoulou,[10] K. Papageorgiou,[154] A. Paramonov,[6] D. Paredes Hernandez,[154] M. A. Parker,[28] K. A. Parker,[139] F. Parodi,[50a,50b] J. A. Parsons,[35] U. Parzefall,[48] E. Pasqualucci,[132a] S. Passaggio,[50a] F. Pastore,[134a,134b,a] Fr. Pastore,[77] G. Pásztor,[29] S. Pataraia,[175] N. D. Patel,[150] J. R. Pater,[84] T. Pauly,[30] J. Pearce,[169] B. Pearson,[113] L. E. Pedersen,[36] M. Pedersen,[119] S. Pedraza Lopez,[167] R. Pedro,[126a,126b] S. V. Peleganchuk,[109,d] D. Pelikan,[166] O. Penc,[127] C. Peng,[33a] H. Peng,[33b] B. Penning,[31] J. Penwell,[61] D. V. Perepelitsa,[25] E. Perez Codina,[159a] M. T. Pérez García-Estañ,[167] L. Perini,[91a,91b] H. Pernegger,[30] S. Perrella,[104a,104b] R. Peschke,[42] V. D. Peshekhonov,[65] K. Peters,[30] R. F. Y. Peters,[84] B. A. Petersen,[30] T. C. Petersen,[36] E. Petit,[42] A. Petridis,[1] C. Petridou,[154] P. Petroff,[117] E. Petrolo,[132a] F. Petrucci,[134a,134b] N. E. Pettersson,[157] R. Pezoa,[32b] P. W. Phillips,[131] G. Piacquadio,[143] E. Pianori,[170]

A. Picazio,[49] E. Piccaro,[76] M. Piccinini,[20a,20b] M. A. Pickering,[120] R. Piegaia,[27] D. T. Pignotti,[111] J. E. Pilcher,[31] A. D. Pilkington,[84] A. W. J. Pin,[84] J. Pina,[126a,126b,126d] M. Pinamonti,[164a,164c,ff] J. L. Pinfold,[3] A. Pingel,[36] S. Pires,[80] H. Pirumov,[42] M. Pitt,[172] C. Pizio,[91a,91b] L. Plazak,[144a] M.-A. Pleier,[25] V. Pleskot,[129] E. Plotnikova,[65] P. Plucinski,[146a,146b] D. Pluth,[64] R. Poettgen,[146a,146b] L. Poggioli,[117] D. Pohl,[21] G. Polesello,[121a] A. Poley,[42] A. Policicchio,[37a,37b] R. Polifka,[158] A. Polini,[20a] C. S. Pollard,[53] V. Polychronakos,[25] K. Pommès,[30] L. Pontecorvo,[132a] B. G. Pope,[90] G. A. Popeneciu,[26c] D. S. Popovic,[13] A. Poppleton,[30] S. Pospisil,[128] K. Potamianos,[15] I. N. Potrap,[65] C. J. Potter,[149] C. T. Potter,[116] G. Poulard,[30] J. Poveda,[30] V. Pozdnyakov,[65] P. Pralavorio,[85] A. Pranko,[15] S. Prasad,[30] S. Prell,[64] D. Price,[84] L. E. Price,[6] M. Primavera,[73a] S. Prince,[87] M. Proissl,[46] K. Prokofiev,[60c] F. Prokoshin,[32b] E. Protopapadaki,[136] S. Protopopescu,[25] J. Proudfoot,[6] M. Przybycien,[38a] E. Ptacek,[116] D. Puddu,[134a,134b] E. Pueschel,[86] D. Puldon,[148] M. Purohit,[25,gg] P. Puzo,[117] J. Qian,[89] G. Qin,[53] Y. Qin,[84] A. Quadt,[54] D. R. Quarrie,[15] W. B. Quayle,[164a,164b] M. Queitsch-Maitland,[84] D. Quilty,[53] S. Raddum,[119] V. Radeka,[25] V. Radescu,[42] S. K. Radhakrishnan,[148] P. Radloff,[116] P. Rados,[88] F. Ragusa,[91a,91b] G. Rahal,[178] S. Rajagopalan,[25] M. Rammensee,[30] C. Rangel-Smith,[166] F. Rauscher,[100] S. Rave,[83] T. Ravenscroft,[53] M. Raymond,[30] A. L. Read,[119] N. P. Readioff,[74] D. M. Rebuzzi,[121a,121b] A. Redelbach,[174] G. Redlinger,[25] R. Reece,[137] K. Reeves,[41] L. Rehnisch,[16] J. Reichert,[122] H. Reisin,[27] C. Rembser,[30] H. Ren,[33a] A. Renaud,[117] M. Rescigno,[132a] S. Resconi,[91a] O. L. Rezanova,[109,d] P. Reznicek,[129] R. Rezvani,[95] R. Richter,[101] S. Richter,[78] E. Richter-Was,[38b] O. Ricken,[21] M. Ridel,[80] P. Rieck,[16] C. J. Riegel,[175] J. Rieger,[54] O. Rifki,[113] M. Rijssenbeek,[148] A. Rimoldi,[121a,121b] L. Rinaldi,[20a] B. Ristić,[49] E. Ritsch,[30] I. Riu,[12] F. Rizatdinova,[114] E. Rizvi,[76] S. H. Robertson,[87,l] A. Robichaud-Veronneau,[87] D. Robinson,[28] J. E. M. Robinson,[42] A. Robson,[53] C. Roda,[124a,124b] S. Roe,[30] O. Røhne,[119] S. Rolli,[161] A. Romaniouk,[98] M. Romano,[20a,20b] S. M. Romano Saez,[34] E. Romero Adam,[167] N. Rompotis,[138] M. Ronzani,[48] L. Roos,[80] E. Ros,[167] S. Rosati,[132a] K. Rosbach,[48] P. Rose,[137] P. L. Rosendahl,[14] O. Rosenthal,[141] V. Rossetti,[146a,146b] E. Rossi,[104a,104b] L. P. Rossi,[50a] J. H. N. Rosten,[28] R. Rosten,[138] M. Rotaru,[26b] I. Roth,[172] J. Rothberg,[138] D. Rousseau,[117] C. R. Royon,[136] A. Rozanov,[85] Y. Rozen,[152] X. Ruan,[145c] F. Rubbo,[143] I. Rubinskiy,[42] V. I. Rud,[99] C. Rudolph,[44] M. S. Rudolph,[158] F. Rühr,[48] A. Ruiz-Martinez,[30] Z. Rurikova,[48] N. A. Rusakovich,[65] A. Ruschke,[100] H. L. Russell,[138] J. P. Rutherfoord,[7] N. Ruthmann,[30] Y. F. Ryabov,[123] M. Rybar,[165] G. Rybkin,[117] N. C. Ryder,[120] A. Ryzhov,[130] A. F. Saavedra,[150] G. Sabato,[107] S. Sacerdoti,[27] A. Saddique,[3] H. F-W. Sadrozinski,[137] R. Sadykov,[65] F. Safai Tehrani,[132a] P. Saha,[108] M. Sahinsoy,[58a] M. Saimpert,[136] T. Saito,[155] H. Sakamoto,[155] Y. Sakurai,[171] G. Salamanna,[134a,134b] A. Salamon,[133a] J. E. Salazar Loyola,[32b] M. Saleem,[113] D. Salek,[107] P. H. Sales De Bruin,[138] D. Salihagic,[101] A. Salnikov,[143] J. Salt,[167] D. Salvatore,[37a,37b] F. Salvatore,[149] A. Salvucci,[60a] A. Salzburger,[30] D. Sammel,[48] D. Sampsonidis,[154] A. Sanchez,[104a,104b] J. Sánchez,[167] V. Sanchez Martinez,[167] H. Sandaker,[119] R. L. Sandbach,[76] H. G. Sander,[83] M. P. Sanders,[100] M. Sandhoff,[175] C. Sandoval,[162] R. Sandstroem,[101] D. P. C. Sankey,[131] M. Sannino,[50a,50b] A. Sansoni,[47] C. Santoni,[34] R. Santonico,[133a,133b] H. Santos,[126a] I. Santoyo Castillo,[149] K. Sapp,[125] A. Sapronov,[65] J. G. Saraiva,[126a,126d] B. Sarrazin,[21] O. Sasaki,[66] Y. Sasaki,[155] K. Sato,[160] G. Sauvage,[5,a] E. Sauvan,[5] G. Savage,[77] P. Savard,[158,e] C. Sawyer,[131] L. Sawyer,[79,o] J. Saxon,[31] C. Sbarra,[20a] A. Sbrizzi,[20a,20b] T. Scanlon,[78] D. A. Scannicchio,[163] M. Scarcella,[150] V. Scarfone,[37a,37b] J. Schaarschmidt,[172] P. Schacht,[101] D. Schaefer,[30] R. Schaefer,[42] J. Schaeffer,[83] S. Schaepe,[21] S. Schaetzel,[58b] U. Schäfer,[83] A. C. Schaffer,[117] D. Schaile,[100] R. D. Schamberger,[148] V. Scharf,[58a] V. A. Schegelsky,[123] D. Scheirich,[129] M. Schernau,[163] C. Schiavi,[50a,50b] C. Schillo,[48] M. Schioppa,[37a,37b] S. Schlenker,[30] K. Schmieden,[30] C. Schmitt,[83] S. Schmitt,[58b] S. Schmitt,[42] B. Schneider,[159a] Y. J. Schnellbach,[74] U. Schnoor,[44] L. Schoeffel,[136] A. Schoening,[58b] B. D. Schoenrock,[90] E. Schopf,[21] A. L. S. Schorlemmer,[54] M. Schott,[83] D. Schouten,[159a] J. Schovancova,[8] S. Schramm,[49] M. Schreyer,[174] N. Schuh,[83] M. J. Schultens,[21] H.-C. Schultz-Coulon,[58a] H. Schulz,[16] M. Schumacher,[48] B. A. Schumm,[137] Ph. Schune,[136] C. Schwanenberger,[84] A. Schwartzman,[143] T. A. Schwarz,[89] Ph. Schwegler,[101] H. Schweiger,[84] Ph. Schwemling,[136] R. Schwienhorst,[90] J. Schwindling,[136] T. Schwindt,[21] F. G. Sciacca,[17] E. Scifo,[117] G. Sciolla,[23] F. Scuri,[124a,124b] F. Scutti,[21] J. Searcy,[89] G. Sedov,[42] E. Sedykh,[123] P. Seema,[21] S. C. Seidel,[105] A. Seiden,[137] F. Seifert,[128] J. M. Seixas,[24a] G. Sekhniaidze,[104a] K. Sekhon,[89] S. J. Sekula,[40] D. M. Seliverstov,[123,a] N. Semprini-Cesari,[20a,20b] C. Serfon,[30] L. Serin,[117] L. Serkin,[164a,164b] T. Serre,[85] M. Sessa,[134a,134b] R. Seuster,[159a] H. Severini,[113] T. Sfiligoj,[75] F. Sforza,[30] A. Sfyrla,[30] E. Shabalina,[54] M. Shamim,[116] L. Y. Shan,[33a] R. Shang,[165] J. T. Shank,[22] M. Shapiro,[15] P. B. Shatalov,[97] K. Shaw,[164a,164b] S. M. Shaw,[84] A. Shcherbakova,[146a,146b] C. Y. Shehu,[149] P. Sherwood,[78] L. Shi,[151,hh] S. Shimizu,[67] C. O. Shimmin,[163] M. Shimojima,[102] M. Shiyakova,[65] A. Shmeleva,[96] D. Shoaleh Saadi,[95] M. J. Shochet,[31] S. Shojaii,[91a,91b] S. Shrestha,[111] E. Shulga,[98] M. A. Shupe,[7] S. Shushkevich,[42] P. Sicho,[127] P. E. Sidebo,[147] O. Sidiropoulou,[174] D. Sidorov,[114] A. Sidoti,[20a,20b] F. Siegert,[44] Dj. Sijacki,[13] J. Silva,[126a,126d] Y. Silver,[153] S. B. Silverstein,[146a] V. Simak,[128] O. Simard,[5] Lj. Simic,[13] S. Simion,[117] E. Simioni,[83]

B. Simmons,[78] D. Simon,[34] P. Sinervo,[158] N. B. Sinev,[116] M. Sioli,[20a,20b] G. Siragusa,[174] A. N. Sisakyan,[65,a] S. Yu. Sivoklokov,[99] J. Sjölin,[146a,146b] T. B. Sjursen,[14] M. B. Skinner,[72] H. P. Skottowe,[57] P. Skubic,[113] M. Slater,[18] T. Slavicek,[128] M. Slawinska,[107] K. Sliwa,[161] V. Smakhtin,[172] B. H. Smart,[46] L. Smestad,[14] S. Yu. Smirnov,[98] Y. Smirnov,[98] L. N. Smirnova,[99,ii] O. Smirnova,[81] M. N. K. Smith,[35] R. W. Smith,[35] M. Smizanska,[72] K. Smolek,[128] A. A. Snesarev,[96] G. Snidero,[76] S. Snyder,[25] R. Sobie,[169,l] F. Socher,[44] A. Soffer,[153] D. A. Soh,[151,hh] G. Sokhrannyi,[75] C. A. Solans,[30] M. Solar,[128] J. Solc,[128] E. Yu. Soldatov,[98] U. Soldevila,[167] A. A. Solodkov,[130] A. Soloshenko,[65] O. V. Solovyanov,[130] V. Solovyev,[123] P. Sommer,[48] H. Y. Song,[33b,z] N. Soni,[1] A. Sood,[15] A. Sopczak,[128] B. Sopko,[128] V. Sopko,[128] V. Sorin,[12] D. Sosa,[58b] M. Sosebee,[8] C. L. Sotiropoulou,[124a,124b] R. Soualah,[164a,164c] A. M. Soukharev,[109,d] D. South,[42] B. C. Sowden,[77] S. Spagnolo,[73a,73b] M. Spalla,[124a,124b] M. Spangenberg,[170] F. Spanò,[77] W. R. Spearman,[57] D. Sperlich,[16] F. Spettel,[101] R. Spighi,[20a] G. Spigo,[30] L. A. Spiller,[88] M. Spousta,[129] R. D. St. Denis,[53,a] A. Stabile,[91a] S. Staerz,[44] J. Stahlman,[122] R. Stamen,[58a] S. Stamm,[16] E. Stanecka,[39] C. Stanescu,[134a] M. Stanescu-Bellu,[42] M. M. Stanitzki,[42] S. Stapnes,[119] E. A. Starchenko,[130] J. Stark,[55] P. Staroba,[127] P. Starovoitov,[58a] R. Staszewski,[39] P. Steinberg,[25] B. Stelzer,[142] H. J. Stelzer,[30] O. Stelzer-Chilton,[159a] H. Stenzel,[52] G. A. Stewart,[53] J. A. Stillings,[21] M. C. Stockton,[87] M. Stoebe,[87] G. Stoicea,[26b] P. Stolte,[54] S. Stonjek,[101] A. R. Stradling,[8] A. Straessner,[44] M. E. Stramaglia,[17] J. Strandberg,[147] S. Strandberg,[146a,146b] A. Strandlie,[119] E. Strauss,[143] M. Strauss,[113] P. Strizenec,[144b] R. Ströhmer,[174] D. M. Strom,[116] R. Stroynowski,[40] A. Strubig,[106] S. A. Stucci,[17] B. Stugu,[14] N. A. Styles,[42] D. Su,[143] J. Su,[125] R. Subramaniam,[79] A. Succurro,[12] S. Suchek,[58a] Y. Sugaya,[118] M. Suk,[128] V. V. Sulin,[96] S. Sultansoy,[4c] T. Sumida,[68] S. Sun,[57] X. Sun,[33a] J. E. Sundermann,[48] K. Suruliz,[149] G. Susinno,[37a,37b] M. R. Sutton,[149] S. Suzuki,[66] M. Svatos,[127] M. Swiatlowski,[143] I. Sykora,[144a] T. Sykora,[129] D. Ta,[48] C. Taccini,[134a,134b] K. Tackmann,[42] J. Taenzer,[158] A. Taffard,[163] R. Tafirout,[159a] N. Taiblum,[153] H. Takai,[25] R. Takashima,[69] H. Takeda,[67] T. Takeshita,[140] Y. Takubo,[66] M. Talby,[85] A. A. Talyshev,[109,d] J. Y. C. Tam,[174] K. G. Tan,[88] J. Tanaka,[155] R. Tanaka,[117] S. Tanaka,[66] B. B. Tannenwald,[111] N. Tannoury,[21] S. Tapia Araya,[32b] S. Tapprogge,[83] S. Tarem,[152] F. Tarrade,[29] G. F. Tartarelli,[91a] P. Tas,[129] M. Tasevsky,[127] T. Tashiro,[68] E. Tassi,[37a,37b] A. Tavares Delgado,[126a,126b] Y. Tayalati,[135d] F. E. Taylor,[94] G. N. Taylor,[88] P. T. E. Taylor,[88] W. Taylor,[159b] F. A. Teischinger,[30] M. Teixeira Dias Castanheira,[76] P. Teixeira-Dias,[77] K. K. Temming,[48] D. Temple,[142] H. Ten Kate,[30] P. K. Teng,[151] J. J. Teoh,[118] F. Tepel,[175] S. Terada,[66] K. Terashi,[155] J. Terron,[82] S. Terzo,[101] M. Testa,[47] R. J. Teuscher,[158,l] T. Theveneaux-Pelzer,[34] J. P. Thomas,[18] J. Thomas-Wilsker,[77] E. N. Thompson,[35] P. D. Thompson,[18] R. J. Thompson,[84] A. S. Thompson,[53] L. A. Thomsen,[176] E. Thomson,[122] M. Thomson,[28] R. P. Thun,[89,a] M. J. Tibbetts,[15] R. E. Ticse Torres,[85] V. O. Tikhomirov,[96,jj] Yu. A. Tikhonov,[109,d] S. Timoshenko,[98] E. Tiouchichine,[85] P. Tipton,[176] S. Tisserant,[85] K. Todome,[157] T. Todorov,[5,a] S. Todorova-Nova,[129] J. Tojo,[70] S. Tokár,[144a] K. Tokushuku,[66] K. Tollefson,[90] E. Tolley,[57] L. Tomlinson,[84] M. Tomoto,[103] L. Tompkins,[143,kk] K. Toms,[105] E. Torrence,[116] H. Torres,[142] E. Torró Pastor,[138] J. Toth,[85,ll] F. Touchard,[85] D. R. Tovey,[139] T. Trefzger,[174] L. Tremblet,[30] A. Tricoli,[30] I. M. Trigger,[159a] S. Trincaz-Duvoid,[80] M. F. Tripiana,[12] W. Trischuk,[158] B. Trocmé,[55] C. Troncon,[91a] M. Trottier-McDonald,[15] M. Trovatelli,[169] L. Truong,[164a,164c] M. Trzebinski,[39] A. Trzupek,[39] C. Tsarouchas,[30] J. C-L. Tseng,[120] P. V. Tsiareshka,[92] D. Tsionou,[154] G. Tsipolitis,[10] N. Tsirintanis,[9] S. Tsiskaridze,[12] V. Tsiskaridze,[48] E. G. Tskhadadze,[51a] K. M. Tsui,[60a] I. I. Tsukerman,[97] V. Tsulaia,[15] S. Tsuno,[66] D. Tsybychev,[148] A. Tudorache,[26b] V. Tudorache,[26b] A. N. Tuna,[57] S. A. Tupputi,[20a,20b] S. Turchikhin,[99,ii] D. Turecek,[128] R. Turra,[91a,91b] A. J. Turvey,[40] P. M. Tuts,[35] A. Tykhonov,[49] M. Tylmad,[146a,146b] M. Tyndel,[131] I. Ueda,[155] R. Ueno,[29] M. Ughetto,[146a,146b] M. Ugland,[14] F. Ukegawa,[160] G. Unal,[30] A. Undrus,[25] G. Unel,[163] F. C. Ungaro,[48] Y. Unno,[66] C. Unverdorben,[100] J. Urban,[144b] P. Urquijo,[88] P. Urrejola,[83] G. Usai,[8] A. Usanova,[62] L. Vacavant,[85] V. Vacek,[128] B. Vachon,[87] C. Valderanis,[83] N. Valencic,[107] S. Valentinetti,[20a,20b] A. Valero,[167] L. Valery,[12] S. Valkar,[129] S. Vallecorsa,[49] J. A. Valls Ferrer,[167] W. Van Den Wollenberg,[107] P. C. Van Der Deijl,[107] R. van der Geer,[107] H. van der Graaf,[107] N. van Eldik,[152] P. van Gemmeren,[6] J. Van Nieuwkoop,[142] I. van Vulpen,[107] M. C. van Woerden,[30] M. Vanadia,[132a,132b] W. Vandelli,[30] R. Vanguri,[122] A. Vaniachine,[6] F. Vannucci,[80] G. Vardanyan,[177] R. Vari,[132a] E. W. Varnes,[7] T. Varol,[40] D. Varouchas,[80] A. Vartapetian,[8] K. E. Varvell,[150] F. Vazeille,[34] T. Vazquez Schroeder,[87] J. Veatch,[7] L. M. Veloce,[158] F. Veloso,[126a,126c] T. Velz,[21] S. Veneziano,[132a] A. Ventura,[73a,73b] D. Ventura,[86] M. Venturi,[169] N. Venturi,[158] A. Venturini,[23] V. Vercesi,[121a] M. Verducci,[132a,132b] W. Verkerke,[107] J. C. Vermeulen,[107] A. Vest,[44] M. C. Vetterli,[142,e] O. Viazlo,[81] I. Vichou,[165] T. Vickey,[139] O. E. Vickey Boeriu,[139] G. H. A. Viehhauser,[120] S. Viel,[15] R. Vigne,[62] M. Villa,[20a,20b] M. Villaplana Perez,[91a,91b] E. Vilucchi,[47] M. G. Vincter,[29] V. B. Vinogradov,[65] I. Vivarelli,[149] F. Vives Vaque,[3] S. Vlachos,[10] D. Vladoiu,[100] M. Vlasak,[128] M. Vogel,[32a] P. Vokac,[128] G. Volpi,[124a,124b] M. Volpi,[88] H. von der Schmitt,[101] H. von Radziewski,[48] E. von Toerne,[21] V. Vorobel,[129] K. Vorobev,[98] M. Vos,[167] R. Voss,[30] J. H. Vossebeld,[74] N. Vranjes,[13]

M. Vranjes Milosavljevic,[13] V. Vrba,[127] M. Vreeswijk,[107] R. Vuillermet,[30] I. Vukotic,[31] Z. Vykydal,[128] P. Wagner,[21] W. Wagner,[175] H. Wahlberg,[71] S. Wahrmund,[44] J. Wakabayashi,[103] J. Walder,[72] R. Walker,[100] W. Walkowiak,[141] C. Wang,[151] F. Wang,[173] H. Wang,[15] H. Wang,[40] J. Wang,[42] J. Wang,[150] K. Wang,[87] R. Wang,[6] S. M. Wang,[151] T. Wang,[21] T. Wang,[35] X. Wang,[176] C. Wanotayaroj,[116] A. Warburton,[87] C. P. Ward,[28] D. R. Wardrope,[78] A. Washbrook,[46] C. Wasicki,[42] P. M. Watkins,[18] A. T. Watson,[18] I. J. Watson,[150] M. F. Watson,[18] G. Watts,[138] S. Watts,[84] B. M. Waugh,[78] S. Webb,[84] M. S. Weber,[17] S. W. Weber,[174] J. S. Webster,[31] A. R. Weidberg,[120] B. Weinert,[61] J. Weingarten,[54] C. Weiser,[48] H. Weits,[107] P. S. Wells,[30] T. Wenaus,[25] T. Wengler,[30] S. Wenig,[30] N. Wermes,[21] M. Werner,[48] P. Werner,[30] M. Wessels,[58a] J. Wetter,[161] K. Whalen,[116] A. M. Wharton,[72] A. White,[8] M. J. White,[1] R. White,[32b] S. White,[124a,124b] D. Whiteson,[163] F. J. Wickens,[131] W. Wiedenmann,[173] M. Wielers,[131] P. Wienemann,[21] C. Wiglesworth,[36] L. A. M. Wiik-Fuchs,[21] A. Wildauer,[101] H. G. Wilkens,[30] H. H. Williams,[122] S. Williams,[107] C. Willis,[90] S. Willocq,[86] A. Wilson,[89] J. A. Wilson,[18] I. Wingerter-Seez,[5] F. Winklmeier,[116] B. T. Winter,[21] M. Wittgen,[143] J. Wittkowski,[100] S. J. Wollstadt,[83] M. W. Wolter,[39] H. Wolters,[126a,126c] B. K. Wosiek,[39] J. Wotschack,[30] M. J. Woudstra,[84] K. W. Wozniak,[39] M. Wu,[55] M. Wu,[31] S. L. Wu,[173] X. Wu,[49] Y. Wu,[89] T. R. Wyatt,[84] B. M. Wynne,[46] S. Xella,[36] D. Xu,[33a] L. Xu,[25] B. Yabsley,[150] S. Yacoob,[145a] R. Yakabe,[67] M. Yamada,[66] D. Yamaguchi,[157] Y. Yamaguchi,[118] A. Yamamoto,[66] S. Yamamoto,[155] T. Yamanaka,[155] K. Yamauchi,[103] Y. Yamazaki,[67] Z. Yan,[22] H. Yang,[33e] H. Yang,[173] Y. Yang,[151] W-M. Yao,[15] Y. C. Yap,[80] Y. Yasu,[66] E. Yatsenko,[5] K. H. Yau Wong,[21] J. Ye,[40] S. Ye,[25] I. Yeletskikh,[65] A. L. Yen,[57] E. Yildirim,[42] K. Yorita,[171] R. Yoshida,[6] K. Yoshihara,[122] C. Young,[143] C. J. S. Young,[30] S. Youssef,[22] D. R. Yu,[15] J. Yu,[8] J. M. Yu,[89] J. Yu,[114] L. Yuan,[67] S. P. Y. Yuen,[21] A. Yurkewicz,[108] I. Yusuff,[28,mm] B. Zabinski,[39] R. Zaidan,[63] A. M. Zaitsev,[130,dd] J. Zalieckas,[14] A. Zaman,[148] S. Zambito,[57] L. Zanello,[132a,132b] D. Zanzi,[88] C. Zeitnitz,[175] M. Zeman,[128] A. Zemla,[38a] Q. Zeng,[143] K. Zengel,[23] O. Zenin,[130] T. Ženiš,[144a] D. Zerwas,[117] D. Zhang,[89] F. Zhang,[173] G. Zhang,[33b] H. Zhang,[33c] J. Zhang,[6] L. Zhang,[48] R. Zhang,[33b,j] X. Zhang,[33d] Z. Zhang,[117] X. Zhao,[40] Y. Zhao,[33d,117] Z. Zhao,[33b] A. Zhemchugov,[65] J. Zhong,[120] B. Zhou,[89] C. Zhou,[45] L. Zhou,[35] L. Zhou,[40] M. Zhou,[148] N. Zhou,[33f] C. G. Zhu,[33d] H. Zhu,[33a] J. Zhu,[89] Y. Zhu,[33b] X. Zhuang,[33a] K. Zhukov,[96] A. Zibell,[174] D. Zieminska,[61] N. I. Zimine,[65] C. Zimmermann,[83] S. Zimmermann,[48] Z. Zinonos,[54] M. Zinser,[83] M. Ziolkowski,[141] L. Živković,[13] G. Zobernig,[173] A. Zoccoli,[20a,20b] M. zur Nedden,[16] G. Zurzolo,[104a,104b] and L. Zwalinski[30]

(ATLAS Collaboration)

[1]*Department of Physics, University of Adelaide, Adelaide, Australia*
[2]*Physics Department, SUNY Albany, Albany, New York, USA*
[3]*Department of Physics, University of Alberta, Edmonton, Alberta, Canada*
[4a]*Department of Physics, Ankara University, Ankara, Turkey*
[4b]*Istanbul Aydin University, Istanbul, Turkey*
[4c]*Division of Physics, TOBB University of Economics and Technology, Ankara, Turkey*
[5]*LAPP, CNRS/IN2P3 and Université Savoie Mont Blanc, Annecy-le-Vieux, France*
[6]*High Energy Physics Division, Argonne National Laboratory, Argonne, Illinois, USA*
[7]*Department of Physics, University of Arizona, Tucson, Arizona, USA*
[8]*Department of Physics, The University of Texas at Arlington, Arlington, Texas, USA*
[9]*Physics Department, University of Athens, Athens, Greece*
[10]*Physics Department, National Technical University of Athens, Zografou, Greece*
[11]*Institute of Physics, Azerbaijan Academy of Sciences, Baku, Azerbaijan*
[12]*Institut de Física d'Altes Energies and Departament de Física de la Universitat Autònoma de Barcelona, Barcelona, Spain*
[13]*Institute of Physics, University of Belgrade, Belgrade, Serbia*
[14]*Department for Physics and Technology, University of Bergen, Bergen, Norway*
[15]*Physics Division, Lawrence Berkeley National Laboratory and University of California, Berkeley, California, USA*
[16]*Department of Physics, Humboldt University, Berlin, Germany*
[17]*Albert Einstein Center for Fundamental Physics and Laboratory for High Energy Physics, University of Bern, Bern, Switzerland*
[18]*School of Physics and Astronomy, University of Birmingham, Birmingham, United Kingdom*
[19a]*Department of Physics, Bogazici University, Istanbul, Turkey*
[19b]*Department of Physics Engineering, Gaziantep University, Gaziantep, Turkey*
[19c]*Department of Physics, Dogus University, Istanbul, Turkey*
[20a]*INFN Sezione di Bologna, Italy*

[20b]*Dipartimento di Fisica e Astronomia, Università di Bologna, Bologna, Italy*

[21]*Physikalisches Institut, University of Bonn, Bonn, Germany*

[22]*Department of Physics, Boston University, Boston, Massachusetts, USA*

[23]*Department of Physics, Brandeis University, Waltham Massachusetts, USA*

[24a]*Universidade Federal do Rio De Janeiro COPPE/EE/IF, Rio de Janeiro, Brazil*

[24b]*Electrical Circuits Department, Federal University of Juiz de Fora (UFJF), Juiz de Fora, Brazil*

[24c]*Federal University of Sao Joao del Rei (UFSJ), Sao Joao del Rei, Brazil*

[24d]*Instituto de Fisica, Universidade de Sao Paulo, Sao Paulo, Brazil*

[25]*Physics Department, Brookhaven National Laboratory, Upton, New York, USA*

[26a]*Transilvania University of Brasov, Brasov, Romania*

[26b]*National Institute of Physics and Nuclear Engineering, Bucharest, Romania*

[26c]*National Institute for Research and Development of Isotopic and Molecular Technologies, Physics Department, Cluj Napoca, Romania*

[26d]*University Politehnica Bucharest, Bucharest, Romania*

[26e]*West University in Timisoara, Timisoara, Romania*

[27]*Departamento de Física, Universidad de Buenos Aires, Buenos Aires, Argentina*

[28]*Cavendish Laboratory, University of Cambridge, Cambridge, United Kingdom*

[29]*Department of Physics, Carleton University, Ottawa, Ontario, Canada*

[30]*CERN, Geneva, Switzerland*

[31]*Enrico Fermi Institute, University of Chicago, Chicago, Illinois, USA*

[32a]*Departamento de Física, Pontificia Universidad Católica de Chile, Santiago, Chile*

[32b]*Departamento de Física, Universidad Técnica Federico Santa María, Valparaíso, Chile*

[33a]*Institute of High Energy Physics, Chinese Academy of Sciences, Beijing, China*

[33b]*Department of Modern Physics, University of Science and Technology of China, Anhui, China*

[33c]*Department of Physics, Nanjing University, Jiangsu, China*

[33d]*School of Physics, Shandong University, Shandong, China*

[33e]*Department of Physics and Astronomy, Shanghai Key Laboratory for Particle Physics and Cosmology, Shanghai Jiao Tong University, Shanghai, China*

[33f]*Physics Department, Tsinghua University, Beijing 100084, China*

[34]*Laboratoire de Physique Corpusculaire, Clermont Université and Université Blaise Pascal and CNRS/IN2P3, Clermont-Ferrand, France*

[35]*Nevis Laboratory, Columbia University, Irvington, New York, USA*

[36]*Niels Bohr Institute, University of Copenhagen, Kobenhavn, Denmark*

[37a]*INFN Gruppo Collegato di Cosenza, Laboratori Nazionali di Frascati, Italy*

[37b]*Dipartimento di Fisica, Università della Calabria, Rende, Italy*

[38a]*AGH University of Science and Technology, Faculty of Physics and Applied Computer Science, Krakow, Poland*

[38b]*Marian Smoluchowski Institute of Physics, Jagiellonian University, Krakow, Poland*

[39]*Institute of Nuclear Physics, Polish Academy of Sciences, Krakow, Poland*

[40]*Physics Department, Southern Methodist University, Dallas, Texas, USA*

[41]*Physics Department, University of Texas at Dallas, Richardson, Texas, USA*

[42]*DESY, Hamburg and Zeuthen, Germany*

[43]*Institut für Experimentelle Physik IV, Technische Universität Dortmund, Dortmund, Germany*

[44]*Institut für Kern- und Teilchenphysik, Technische Universität Dresden, Dresden, Germany*

[45]*Department of Physics, Duke University, Durham, North Carolina, USA*

[46]*SUPA—School of Physics and Astronomy, University of Edinburgh, Edinburgh, United Kingdom*

[47]*INFN Laboratori Nazionali di Frascati, Frascati, Italy*

[48]*Fakultät für Mathematik und Physik, Albert-Ludwigs-Universität, Freiburg, Germany*

[49]*Section de Physique, Université de Genève, Geneva, Switzerland*

[50a]*INFN Sezione di Genova, Italy*

[50b]*Dipartimento di Fisica, Università di Genova, Genova, Italy*

[51a]*E. Andronikashvili Institute of Physics, Iv. Javakhishvili Tbilisi State University, Tbilisi, Georgia*

[51b]*High Energy Physics Institute, Tbilisi State University, Tbilisi, Georgia*

[52]*II Physikalisches Institut, Justus-Liebig-Universität Giessen, Giessen, Germany*

[53]*SUPA—School of Physics and Astronomy, University of Glasgow, Glasgow, United Kingdom*

[54]*II Physikalisches Institut, Georg-August-Universität, Göttingen, Germany*

[55]*Laboratoire de Physique Subatomique et de Cosmologie, Université Grenoble-Alpes, CNRS/IN2P3, Grenoble, France*

[56]*Department of Physics, Hampton University, Hampton, Virginia, USA*

[57]*Laboratory for Particle Physics and Cosmology, Harvard University, Cambridge, Massachusetts, USA*

[58a]*Kirchhoff-Institut für Physik, Ruprecht-Karls-Universität Heidelberg, Heidelberg, Germany*
[58b]*Physikalisches Institut, Ruprecht-Karls-Universität Heidelberg, Heidelberg, Germany*
[58c]*ZITI Institut für technische Informatik, Ruprecht-Karls-Universität Heidelberg, Mannheim, Germany*
[59]*Faculty of Applied Information Science, Hiroshima Institute of Technology, Hiroshima, Japan*
[60a]*Department of Physics, The Chinese University of Hong Kong, Shatin, N.T., Hong Kong, China*
[60b]*Department of Physics, The University of Hong Kong, Hong Kong, China*
[60c]*Department of Physics, The Hong Kong University of Science and Technology, Clear Water Bay, Kowloon, Hong Kong, China*
[61]*Department of Physics, Indiana University, Bloomington IN, United States of America*
[62]*Institut für Astro- und Teilchenphysik, Leopold-Franzens-Universität, Innsbruck, Austria*
[63]*University of Iowa, Iowa City, Iowa, USA*
[64]*Department of Physics and Astronomy, Iowa State University, Ames, Iowa, USA*
[65]*Joint Institute for Nuclear Research, JINR Dubna, Dubna, Russia*
[66]*KEK, High Energy Accelerator Research Organization, Tsukuba, Japan*
[67]*Graduate School of Science, Kobe University, Kobe, Japan*
[68]*Faculty of Science, Kyoto University, Kyoto, Japan*
[69]*Kyoto University of Education, Kyoto, Japan*
[70]*Department of Physics, Kyushu University, Fukuoka, Japan*
[71]*Instituto de Física La Plata, Universidad Nacional de La Plata and CONICET, La Plata, Argentina*
[72]*Physics Department, Lancaster University, Lancaster, United Kingdom*
[73a]*INFN Sezione di Lecce, Italy*
[73b]*Dipartimento di Matematica e Fisica, Università del Salento, Lecce, Italy*
[74]*Oliver Lodge Laboratory, University of Liverpool, Liverpool, United Kingdom*
[75]*Department of Physics, Jožef Stefan Institute and University of Ljubljana, Ljubljana, Slovenia*
[76]*School of Physics and Astronomy, Queen Mary University of London, London, United Kingdom*
[77]*Department of Physics, Royal Holloway University of London, Surrey, United Kingdom*
[78]*Department of Physics and Astronomy, University College London, London, United Kingdom*
[79]*Louisiana Tech University, Ruston, Louisiana, USA*
[80]*Laboratoire de Physique Nucléaire et de Hautes Energies, UPMC and Université Paris-Diderot and CNRS/IN2P3, Paris, France*
[81]*Fysiska institutionen, Lunds universitet, Lund, Sweden*
[82]*Departamento de Fisica Teorica C-15, Universidad Autonoma de Madrid, Madrid, Spain*
[83]*Institut für Physik, Universität Mainz, Mainz, Germany*
[84]*School of Physics and Astronomy, University of Manchester, Manchester, United Kingdom*
[85]*CPPM, Aix-Marseille Université and CNRS/IN2P3, Marseille, France*
[86]*Department of Physics, University of Massachusetts, Amherst, Massachusetts, USA*
[87]*Department of Physics, McGill University, Montreal, Québec, Canada*
[88]*School of Physics, University of Melbourne, Victoria, Australia*
[89]*Department of Physics, The University of Michigan, Ann Arbor, Michigan, USA*
[90]*Department of Physics and Astronomy, Michigan State University, East Lansing, Michigan, USA*
[91a]*INFN Sezione di Milano, Italy*
[91b]*Dipartimento di Fisica, Università di Milano, Milano, Italy*
[92]*B. I. Stepanov Institute of Physics, National Academy of Sciences of Belarus, Minsk, Republic of Belarus*
[93]*National Scientific and Educational Centre for Particle and High Energy Physics, Minsk, Republic of Belarus*
[94]*Department of Physics, Massachusetts Institute of Technology, Cambridge, Massachusetts, USA*
[95]*Group of Particle Physics, University of Montreal, Montreal, Québec, Canada*
[96]*P. N. Lebedev Institute of Physics, Academy of Sciences, Moscow, Russia*
[97]*Institute for Theoretical and Experimental Physics (ITEP), Moscow, Russia*
[98]*National Research Nuclear University, MEPhI, Moscow, Russia*
[99]*D. V. Skobeltsyn Institute of Nuclear Physics, M. V. Lomonosov Moscow State University, Moscow, Russia*
[100]*Fakultät für Physik, Ludwig-Maximilians-Universität München, München, Germany*
[101]*Max-Planck-Institut für Physik, Werner-Heisenberg-Institut, München, Germany*
[102]*Nagasaki Institute of Applied Science, Nagasaki, Japan*
[103]*Graduate School of Science and Kobayashi-Maskawa Institute, Nagoya University, Nagoya, Japan*
[104a]*INFN Sezione di Napoli, Italy*
[104b]*Dipartimento di Fisica, Università di Napoli, Napoli, Italy*
[105]*Department of Physics and Astronomy, University of New Mexico, Albuquerque, New Mexico, USA*

[106]Institute for Mathematics, Astrophysics and Particle Physics, Radboud University Nijmegen/Nikhef, Nijmegen, Netherlands

[107]Nikhef National Institute for Subatomic Physics and University of Amsterdam, Amsterdam, Netherlands

[108]Department of Physics, Northern Illinois University, DeKalb, Illinois, USA

[109]Budker Institute of Nuclear Physics, SB RAS, Novosibirsk, Russia

[110]Department of Physics, New York University, New York, New York, USA

[111]Ohio State University, Columbus, Ohio, USA

[112]Faculty of Science, Okayama University, Okayama, Japan

[113]Homer L. Dodge Department of Physics and Astronomy, University of Oklahoma, Norman, Oklahoma, USA

[114]Department of Physics, Oklahoma State University, Stillwater, Oklahoma, USA

[115]Palacký University, RCPTM, Olomouc, Czech Republic

[116]Center for High Energy Physics, University of Oregon, Eugene, Oregon, USA

[117]LAL, Université Paris-Sud and CNRS/IN2P3, Orsay, France

[118]Graduate School of Science, Osaka University, Osaka, Japan

[119]Department of Physics, University of Oslo, Oslo, Norway

[120]Department of Physics, Oxford University, Oxford, United Kingdom

[121a]INFN Sezione di Pavia, Italy

[121b]Dipartimento di Fisica, Università di Pavia, Pavia, Italy

[122]Department of Physics, University of Pennsylvania, Philadelphia, Pennsylvania, USA

[123]National Research Centre "Kurchatov Institute", B. P. Konstantinov Petersburg Nuclear Physics Institute, St. Petersburg, Russia

[124a]INFN Sezione di Pisa, Italy

[124b]Dipartimento di Fisica E. Fermi, Università di Pisa, Pisa, Italy

[125]Department of Physics and Astronomy, University of Pittsburgh, Pittsburgh, Pennsylvania, USA

[126a]Laboratório de Instrumentação e Física Experimental de Partículas—LIP, Lisboa, Portugal

[126b]Faculdade de Ciências, Universidade de Lisboa, Lisboa, Portugal

[126c]Department of Physics, University of Coimbra, Coimbra, Portugal

[126d]Centro de Física Nuclear da Universidade de Lisboa, Lisboa, Portugal

[126e]Departamento de Fisica, Universidade do Minho, Braga, Portugal

[126f]Departamento de Fisica Teorica y del Cosmos and CAFPE, Universidad de Granada, Granada, Spain

[126g]Dep Fisica and CEFITEC of Faculdade de Ciencias e Tecnologia, Universidade Nova de Lisboa, Caparica, Portugal

[127]Institute of Physics, Academy of Sciences of the Czech Republic, Praha, Czech Republic

[128]Czech Technical University in Prague, Praha, Czech Republic

[129]Faculty of Mathematics and Physics, Charles University in Prague, Praha, Czech Republic

[130]State Research Center Institute for High Energy Physics (Protvino), NRC KI, Russia

[131]Particle Physics Department, Rutherford Appleton Laboratory, Didcot, United Kingdom

[132a]INFN Sezione di Roma, Italy

[132b]Dipartimento di Fisica, Sapienza Università di Roma, Roma, Italy

[133a]INFN Sezione di Roma Tor Vergata, Italy

[133b]Dipartimento di Fisica, Università di Roma Tor Vergata, Roma, Italy

[134a]INFN Sezione di Roma Tre, Italy

[134b]Dipartimento di Matematica e Fisica, Università Roma Tre, Roma, Italy

[135a]Faculté des Sciences Ain Chock, Réseau Universitaire de Physique des Hautes Energies—Université Hassan II, Casablanca, Morocco

[135b]Centre National de l'Energie des Sciences Techniques Nucleaires, Rabat, Morocco

[135c]Faculté des Sciences Semlalia, Université Cadi Ayyad, LPHEA-Marrakech, Morocco

[135d]Faculté des Sciences, Université Mohamed Premier and LPTPM, Oujda, Morocco

[135e]Faculté des sciences, Université Mohammed V, Rabat, Morocco

[136]DSM/IRFU (Institut de Recherches sur les Lois Fondamentales de l'Univers), CEA Saclay (Commissariat à l'Energie Atomique et aux Energies Alternatives), Gif-sur-Yvette, France

[137]Santa Cruz Institute for Particle Physics, University of California Santa Cruz, Santa Cruz, California, USA

[138]Department of Physics, University of Washington, Seattle, Washington, USA

[139]Department of Physics and Astronomy, University of Sheffield, Sheffield, United Kingdom

[140]Department of Physics, Shinshu University, Nagano, Japan

[141]Fachbereich Physik, Universität Siegen, Siegen, Germany

[142]Department of Physics, Simon Fraser University, Burnaby, British Columbia, Canada

[143]SLAC National Accelerator Laboratory, Stanford, California, USA

[144a]*Faculty of Mathematics, Physics & Informatics, Comenius University, Bratislava, Slovak Republic*
[144b]*Department of Subnuclear Physics, Institute of Experimental Physics of the Slovak Academy of Sciences, Kosice, Slovak Republic*
[145a]*Department of Physics, University of Cape Town, Cape Town, South Africa*
[145b]*Department of Physics, University of Johannesburg, Johannesburg, South Africa*
[145c]*School of Physics, University of the Witwatersrand, Johannesburg, South Africa*
[146a]*Department of Physics, Stockholm University, Sweden*
[146b]*The Oskar Klein Centre, Stockholm, Sweden*
[147]*Physics Department, Royal Institute of Technology, Stockholm, Sweden*
[148]*Departments of Physics & Astronomy and Chemistry, Stony Brook University, Stony Brook, New York, USA*
[149]*Department of Physics and Astronomy, University of Sussex, Brighton, United Kingdom*
[150]*School of Physics, University of Sydney, Sydney, Australia*
[151]*Institute of Physics, Academia Sinica, Taipei, Taiwan*
[152]*Department of Physics, Technion: Israel Institute of Technology, Haifa, Israel*
[153]*Raymond and Beverly Sackler School of Physics and Astronomy, Tel Aviv University, Tel Aviv, Israel*
[154]*Department of Physics, Aristotle University of Thessaloniki, Thessaloniki, Greece*
[155]*International Center for Elementary Particle Physics and Department of Physics, The University of Tokyo, Tokyo, Japan*
[156]*Graduate School of Science and Technology, Tokyo Metropolitan University, Tokyo, Japan*
[157]*Department of Physics, Tokyo Institute of Technology, Tokyo, Japan*
[158]*Department of Physics, University of Toronto, Toronto, Ontario, Canada*
[159a]*TRIUMF, Vancouver, British Columbia, Canada*
[159b]*Department of Physics and Astronomy, York University, Toronto, Ontario, Canada*
[160]*Faculty of Pure and Applied Sciences, and Center for Integrated Research in Fundamental Science and Engineering, University of Tsukuba, Tsukuba, Japan*
[161]*Department of Physics and Astronomy, Tufts University, Medford, Massachusetts, USA*
[162]*Centro de Investigaciones, Universidad Antonio Narino, Bogota, Colombia*
[163]*Department of Physics and Astronomy, University of California Irvine, Irvine, California, USA*
[164a]*INFN Gruppo Collegato di Udine, Sezione di Trieste, Udine, Italy*
[164b]*ICTP, Trieste, Italy*
[164c]*Dipartimento di Chimica, Fisica e Ambiente, Università di Udine, Udine, Italy*
[165]*Department of Physics, University of Illinois, Urbana, Illinois, USA*
[166]*Department of Physics and Astronomy, University of Uppsala, Uppsala, Sweden*
[167]*Instituto de Física Corpuscular (IFIC) and Departamento de Física Atómica, Molecular y Nuclear and Departamento de Ingeniería Electrónica and Instituto de Microelectrónica de Barcelona (IMB-CNM), University of Valencia and CSIC, Valencia, Spain*
[168]*Department of Physics, University of British Columbia, Vancouver, British Columbia, Canada*
[169]*Department of Physics and Astronomy, University of Victoria, Victoria, British Columbia, Canada*
[170]*Department of Physics, University of Warwick, Coventry, United Kingdom*
[171]*Waseda University, Tokyo, Japan*
[172]*Department of Particle Physics, The Weizmann Institute of Science, Rehovot, Israel*
[173]*Department of Physics, University of Wisconsin, Madison WI, United States of America*
[174]*Fakultät für Physik und Astronomie, Julius-Maximilians-Universität, Würzburg, Germany*
[175]*Fachbereich C Physik, Bergische Universität Wuppertal, Wuppertal, Germany*
[176]*Department of Physics, Yale University, New Haven, Connecticut, USA*
[177]*Yerevan Physics Institute, Yerevan, Armenia*
[178]*Centre de Calcul de l'Institut National de Physique, Nucléaire et de Physique des Particules (IN2P3), Villeurbanne, France*

[a]Deceased.
[b]Also at Department of Physics, King's College London, London, United Kingdom.
[c]Also at Institute of Physics, Azerbaijan Academy of Sciences, Baku, Azerbaijan.
[d]Also at Novosibirsk State University, Novosibirsk, Russia.
[e]Also at TRIUMF, Vancouver BC, Canada.
[f]Also at Department of Physics, California State University, Fresno CA, United States of America.
[g]Also at Department of Physics, University of Fribourg, Fribourg, Switzerland.
[h]Also at Departamento de Fisica e Astronomia, Faculdade de Ciencias, Universidade do Porto, Portugal.
[i]Also at Tomsk State University, Tomsk, Russia.
[j]Also at CPPM, Aix-Marseille Université and CNRS/IN2P3, Marseille, France.

[k]Also at Universita di Napoli Parthenope, Napoli, Italy.
[l]Also at Institute of Particle Physics (IPP), Canada.
[m]Also at Particle Physics Department, Rutherford Appleton Laboratory, Didcot, United Kingdom.
[n]Also at Department of Physics, St. Petersburg State Polytechnical University, St. Petersburg, Russia.
[o]Also at Louisiana Tech University, Ruston LA, United States of America.
[p]Also at Institucio Catalana de Recerca i Estudis Avancats, ICREA, Barcelona, Spain.
[q]Also at Department of Physics, The University of Michigan, Ann Arbor MI, United States of America.
[r]Also at Graduate School of Science, Osaka University, Osaka, Japan.
[s]Also at Department of Physics, National Tsing Hua University, Taiwan.
[t]Also at Department of Physics, The University of Texas at Austin, Austin TX, United States of America.
[u]Also at Institute of Theoretical Physics, Ilia State University, Tbilisi, Georgia.
[v]Also at CERN, Geneva, Switzerland.
[w]Also at Georgian Technical University (GTU),Tbilisi, Georgia.
[x]Also at Manhattan College, New York NY, United States of America.
[y]Also at Hellenic Open University, Patras, Greece.
[z]Also at Institute of Physics, Academia Sinica, Taipei, Taiwan.
[aa]Also at LAL, Université Paris-Sud and CNRS/IN2P3, Orsay, France.
[bb]Also at Academia Sinica Grid Computing, Institute of Physics, Academia Sinica, Taipei, Taiwan.
[cc]Also at School of Physics, Shandong University, Shandong, China.
[dd]Also at Moscow Institute of Physics and Technology State University, Dolgoprudny, Russia.
[ee]Also at Section de Physique, Université de Genève, Geneva, Switzerland.
[ff]Also at International School for Advanced Studies (SISSA), Trieste, Italy.
[gg]Also at Department of Physics and Astronomy, University of South Carolina, Columbia SC, United States of America.
[hh]Also at School of Physics and Engineering, Sun Yat-sen University, Guangzhou, China.
[ii]Also at Faculty of Physics, M. V. Lomonosov Moscow State University, Moscow, Russia.
[jj]Also at National Research Nuclear University MEPhI, Moscow, Russia.
[kk]Also at Department of Physics, Stanford University, Stanford CA, United States of America.
[ll]Also at Institute for Particle and Nuclear Physics, Wigner Research Centre for Physics, Budapest, Hungary.
[mm]Also at University of Malaya, Department of Physics, Kuala Lumpur, Malaysia.